Clopidogrel Loaded Albumin Nanoparticles for the Management of Atherosclerosis: Preparation and Optimization by Box-Behnken Design

Article *in* Advances in Pharmacology and Pharmacy · July 2024

DOI: 10.13189/app.2024.120401

5 authors, including:

Umadevi Sankararajan
Vels University
41 PUBLICATIONS **181** CITATIONS

SEE PROFILE

Dr. Josephine Leno Jenita Joseph
Dayananda Sagar Institutions
47 PUBLICATIONS **562** CITATIONS

SEE PROFILE

Advances in Pharmacology and Pharmacy 12(4): 265-288, 2024 http://www.hrpub.org
DOI: 10.13189/app.2024.120401

Clopidogrel Loaded Albumin Nanoparticles for the Management of Atherosclerosis: Preparation and Optimization by Box-Behnken Design

Archana MR[1], Seema S Rathore[1], S. Umadevi[2], J. Josephine Leno Jenita[1,*]

[1]Department of Pharmaceutics, College of Pharmaceutical Sciences, Dayananda Sagar University, India
[2]Department of Pharmaceutics, School of Pharmaceutical Sciences, Vels Institute of Science Technology and Advanced Studies, Pallavaram, Tamil Nadu, India

Received August 5, 2023; Revised January 6, 2024; Accepted March 19, 2024

Cite This Paper in the Following Citation Styles

(a): *[1] Archana MR, Seema S Rathore, S. Umadevi, J. Josephine Leno Jenita , "Clopidogrel Loaded Albumin Nanoparticles for the Management of Atherosclerosis: Preparation and Optimization by Box-Behnken Design," Advances in Pharmacology and Pharmacy, Vol. 12, No. 4, pp. 265 - 288, 2024. DOI: 10.13189/app.2024.120401.*

(b): *Archana MR, Seema S Rathore, S. Umadevi, J. Josephine Leno Jenita (2024). Clopidogrel Loaded Albumin Nanoparticles for the Management of Atherosclerosis: Preparation and Optimization by Box-Behnken Design. Advances in Pharmacology and Pharmacy, 12(4), 265 - 288. DOI: 10.13189/app.2024.120401.*

Abstract This study aimed to formulate and optimize the clopidogrel loaded bovine serum albumin nanoparticles as a sustained drug delivery system for effective management of atherosclerosis. The antiplatelet drug clopidogrel has poor water solubility and oral availability of ≤ 50% with rapid first-pass metabolism. The clopidogrel loaded albumin nanoparticles were successfully prepared by the desolvation technique and the Box-Behnken quadratic model which was employed for optimization. For the initial study, the concentration of BSA, 4% v/v glutaraldehyde, and the pH of the polymeric solution were modified and the stirring speed, stirring time, and quantity of drug were kept constant. The process yield, PDI and drug loading were characterized. As the preliminary formulation had higher PDI, particle size and lower drug loading, the formulation was further subjected to optimization by Box-Behnken design. The Box-Behnken quadratic model was employed to optimize the formulation and to study the effect of independent variables like X_1 (Polymer concentration), X_2 (pH), and X_3 (Cross-linking hours) on dependent variables like particle size, PDI, and drug loading. The particle morphologies and zeta potential of optimized CLP-BSA NPs were examined. The efficiency of nanoparticles was confirmed in the Wister albino rats, and the animals treated with CLP-BSA NPs showed prolonged clotting and bleeding time compared to control and clopidogrel drug solution-treated groups.

Keywords Bovine Serum Albumin, Clopidogrel, Atherosclerosis, Box-Behnken Design

1. Introduction

According to WHO estimates, 17.9 million people around the world died in 2016 as a result of cardiovascular disease (CVD), accounting for 31% of all fatalities. Heart attack and stroke deaths accounted for 85% of these fatalities. Additionally, CVD account for 45% of deaths in people aged 40 to 69 [1,2]. Atherosclerosis is one of the conditions lead to cardiovascular disease (CVD) which causes the fatty deposits to clog the arteries [3]. In atherosclerosis, the arteries are usually hard in nature due to formation of the plaque on the inner wall [4,5]. These results in poor blood flow, which causes angina and walking-related leg cramps. A fatal heart attack, stroke, or other severe consequence is possible [6,7]. Clopidogrel (CLP) (Figure 1), a thienopyridine drug chemically related to ticlopidine, prevents platelet aggregation irreversibly by blocking the P2Y12 receptor on the platelet membrane and consequently preventing the ADP-induced platelet aggregation [8]. CLP is a drug of choice for management of atherosclerosis, but it has a limited bio-availability of about 50%. This is because it undergoes first-pass

metabolism in the liver, where it creates a thiol metabolite that is rapidly eliminated. The absorption of CLP is pH-dependent; it gets absorbed at acidic pH and precipitates at basic pH; it has low water solubility, and quick first pass metabolism [9, 10, 11]. Nanotechnology-based drug delivery systems enable medications to overcome their drawbacks, and they improve the performance of traditional drugs by leveraging their size and decreasing dose requirements. These systems distribute medications selectively to their targets and provide more selective and effective systems with fewer adverse effects [12].

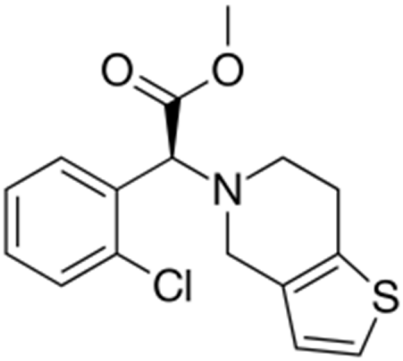

Figure 1. Chemical structure of Clopidogrel

The performance of nanoparticles (NPs) depends on surface charge, surface modification, dimensionality, and hydrophobicity, which can impact the material's reactivity and physical and chemical properties. Nanocarriers with optimum physical, chemical, and biological features can reach the cells, and other bulkier materials would not be taken up or expelled from the body. Nanocarriers may have an impact on cellular responses because their smaller sizes (50-300nm) permit contact with biomolecules within or on the surface of cells [13].

CLP was chosen as the appropriate drug for the current investigation since considerable research on nanoparticles for management of atherosclerosis has not yet been done. In this study, the nanoparticles were formulated and optimized using Box-Behnken design (BBD) [9]. The particle size and size distribution, surface charge, particle shape, thermal behavior, and interaction of prepared CLP-BSA NPs were evaluated. Furthermore, the effects of prepared CLP-BSA NPs on bleeding and clotting time were examined in Wister albino rats.

2. Materials and Methods

2.1. Materials

Clopidogrel hydrogen sulphate was gifted by Sterile-Gene Life Sciences (P) Ltd, Puducherry. Bovine serum albumin (BSA) was procured from Sigma Aldrich, Bangalore. Glutaraldehyde, Sodium hydroxide and Ethanol were purchased from Spectrochem Private Ltd, Bangalore. The chemicals & solvents used were of analytical grade.

2.2. Preparation and Optimization of Clopidogrel-loaded BSA Nanoparticles

The CLP-BSA NPs were prepared by desolvation method [14, 15]. BSA was dissolved in 5ml of water and the pH of the solution was adjusted using 0.1 N NaOH. CLP was dissolved separately in 2 ml of ethanol. Using a syringe and a steady stirring rate (550 rpm) at room temperature, the drug solution was infused into the polymeric solution drop by drop at a rate of 2 ml per minute. To the aforementioned mixture, ethanol was added until the solution turned turbid, signifying the formation of nanoparticles. Later, 4% glutaraldehyde was added to the mixture to stabilize it. Overnight, the solution was left to stir. After stirring for an entire night, the mixture was centrifuged for 15 minutes at 20,000 rpm at 25°C. The sediment was collected, washed with water, and freeze-dried with 5% Sorbitol as a cryoprotectant to produce fine NP powder, which was then kept in a desiccator at 4°C (Figure 2). By applying the Response Surface Model (RSM), 17 formulations were prepared and characterized. Figure 2 indicates the method of nanoparticle preparation.

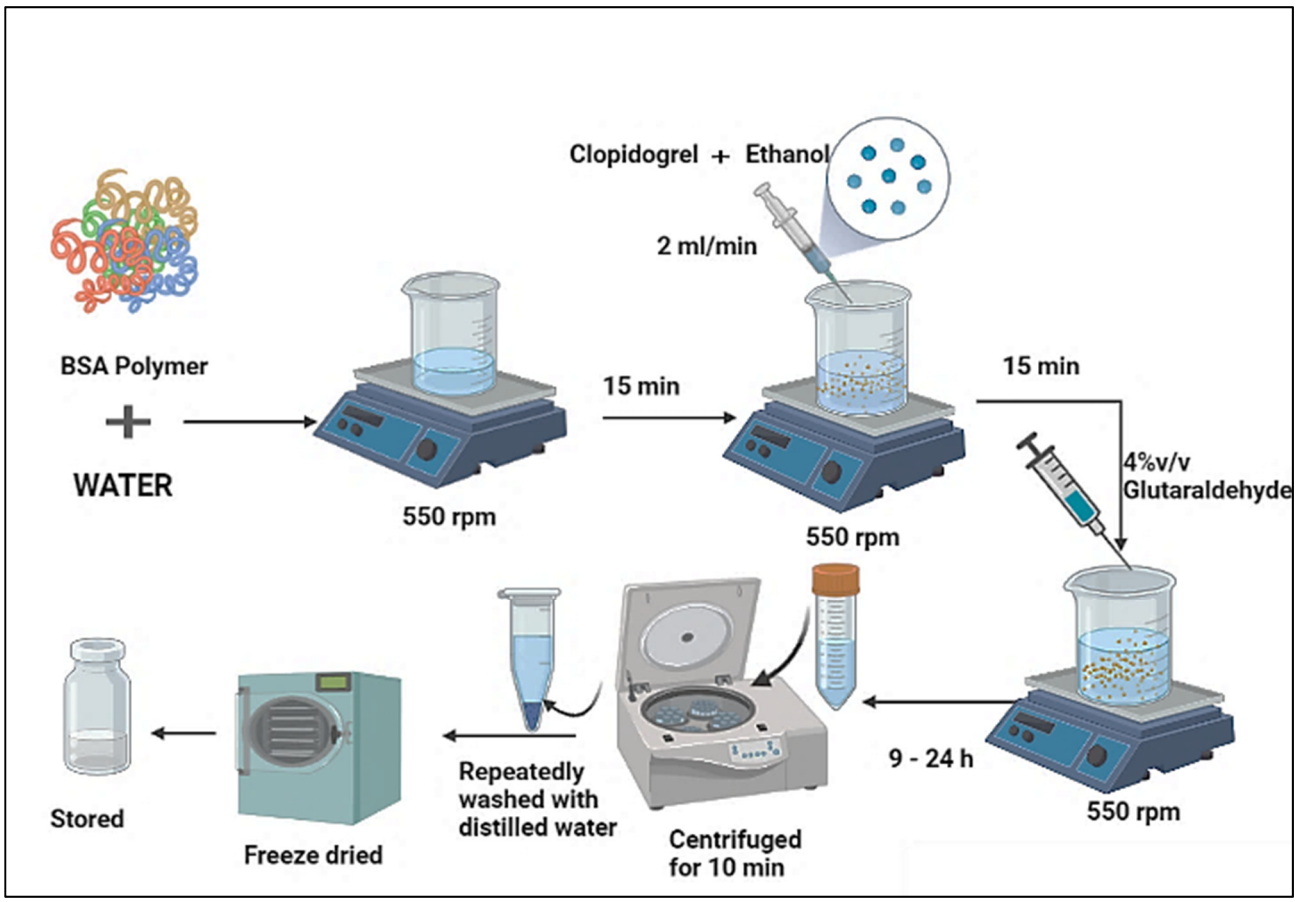

Figure 2. Schematic representation of the method used for the preparation of CLP-BSA NPs

2.3. Experimental Design

The choice of dependent and independent variables was done based on the initial trial process. In the initial stage, the NPs were prepared by varying one factor at a time. At pH 8, polymer and drug ratio of 2:1, and 1.5 ml of 4% v/v glutaraldehyde solution had better process yield, but the effect on particle size and size distribution analysis was undesirable. Hence, to produce NPs with minimized particle size and its distribution and high drug loading, BBD was used.

The Design-Expert Software, version (15) was used to optimize CLP-BSA NPs using a 17-run, 3-factor, and 3-level BBD. The independent variables selected based on the preliminary study were the polymer concentration (X_1), pH of the polymeric solution (X_2) and cross-linking time in h (X_3) (Table 1) and the effects of these were studied on Particle size, PDI, and drug loading which were selected as dependent variables. An ANOVA analysis was conducted on the response variables, which is always needed to assess the relevance and suitability of the mathematical models that RSM suggests [16]. Each parameter underwent an F-test (p-0.05) evaluation, and responses were put via numerous regression studies. The model was found to be significant if the p value was less than 0.05. The R^2 value was used to determine the variance of a response variable which is further explained by the process variable [17].

$$Y = b_0 + b_1X_1 + b_2X_2 + b_3X_3 + b_4X_1^2 + b_5X_1X_2 + b_6X_1X_3 + b_7X_2^2 + b_8X_2X_3 + b_9X_3^2 + E$$

Table 1. Selection of dependent variables and their levels for the Box-Behnken design

Symbol	Variable	Low	Medium	High
A	Polymer concentration	10 mg	20 mg	30 mg
B	pH	7	8	9
C	Cross linking time	9 h	16.5 h	24 h

2.4. Characterization of the Prepared CLP-BSA NPs

2.4.1. Compatibility Studies

The Shimadzu FT-IR Spectrophotometer was used to detect the interaction between drug (CLP) and polymer (BSA). The KBr pellet method was used to study the compatibility. The samples were placed in a separate pellet maker and compressed at a rate of 10 kg/cm^2 using a pellet press to form pellets. The pellets were placed in a sample holder and scanned in the Shimadzu FT-IR spectrophotometer at 4000 cm^{-1} to 400 cm^{-1}.

The DSC thermograms of CLP and CLP-BSA NPs were obtained by differential scanning calorimeter (Universal V 4.5A TA). The 10 mg of the sample, was enclosed in the

aluminium pans. It was heated at a rate of 10°C/min, between 30 and 400°C, under an inert nitrogen environment, to record the DSC thermograms.

2.4.2. Determination of Process Yield

The process yield of CLP-BSA NPs was calculated by considering the weight of final product after drying, the initial amount of the drug and the polymer used for the preparation of NPs [18]. The process yield was calculated by the following equation.

$$Process\ \ yield\ \ (\%) = \frac{Practical\ \ yield}{Theoritical\ \ yield} \times 100$$

2.4.3. Determination of Drug Loading

UV-Visible spectroscopy was used to determine the amount of CLP loaded in the NPs at 220nm. The NPs equivalent 100mg CLP was completely extracted using pH 7.4 phosphate buffer by centrifugation process for 10 minutes at 10000 rpm [19]. The drug loading was determined by using the following formula.

$$\%\ \ Drug\ \ loading = \frac{Actual\ \ drug\ \ content}{Weight\ \ of\ \ NPs\ \ taken} \times 100$$

2.4.4. *In vitro* Drug Release Study

The *in vitro* drug release of CLP-BSA NPs was carried out by the dialysis bag method [20]. The NPs were placed in the dialysis membrane. 1 ml of pH 7.4 phosphate buffer was added and tied at both ends. The dialysis bag was immersed in 100 ml of pH 7.4 phosphate buffer, allowing it to come into complete contact with the dissolution media, and stirred at 500 rpm at room temperature. The dissolution medium was removed at predetermined time intervals and was replaced with fresh dissolution medium to maintain sink condition. The amount of CLP released in the receptor media at different time intervals was determined by measuring the absorbance at 220 nm using a UV-spectrophotometer.

2.5. Evaluation of CLP-BSA NPs

2.5.1. Particle Size Analysis

The particle size and PDI of the prepared CLP-BSA NPs were measured by laser light scattering method [19] using Malvern Zetasizer Nano ZS (Malvern Instruments, UK).

2.5.2. Zeta Potential

The zeta potential of the formulated CLP-BSA NPs was determined using the HORIBA SZ- 100 dynamic light scattering method [19] (HORIBA Instruments, Japan).

2.5.3. Surface Morphology

The surface morphology of CLP-BSA NPs was determined by the Transmission Electron Microscopy (TEM) method. A Philips CM 120 electron microscope with a 100 kV accelerating voltage was used to take the TEM pictures. Here, 2% ammonium molybdate solution was used to initially stain the samples. Later, images were captured after the CLP-BSA NP suspension was put onto a copper grid that had been coated with carbon.

2.5.4. Release Kinetics

The data from *in vitro* study was fitted to various kinetic models including zero order, first order, the Higuchi model, and the Korsmeyer-Peppas model [20, 21].

2.5.5. Animal Studies

The animals the study used were Wister albino rats (DSU/M.Pharm/ IAEC/78/2021-22). They were divided into 3 groups, each group containing 6 animals. The first group of albino rats was labelled as control and they received 0.9% w/v normal saline; the second group was labelled as free pure drug and received a pure form of CLP and the third group received CLP-BSA NPs. The formulations were injected by intra venous route through a tail vein for 7 days. The bleeding time and blood clotting efficiency were monitored and recorded [22,23].

2.6. Bleeding Time Determination

The tail transection method was used to measure the bleeding time [23]. Here, the tail was transacted and the bleeding was noted for a maximum of 900 sec. Once the bleeding would halt, that time was considered as the end point. But, if bleeding restarts within 30 sec, then bleeding time is recorded till the bleeding stops.

2.7. Clotting Time Determination

Clotting time was determined by capillary glass method [23]. In this method, the blood is withdrawn from the retro-orbital route in a capillary tube. A tiny piece of the glass tube is wrecked off every 30 seconds until a fine thread of clotted blood is observed. The time taken for a fine layer of thread to appear is considered as the clotting time.

3. Results and Discussion

3.1. Preparation

Seventeen batches of CLP-BSA-NPS were prepared by desolvation method (Table 2). The polymer BSA was utilized in the preparation because it has great biocompatibility, long-term storage stability, and well-defined nano-structure production capabilities [24,25]. Sodium hydroxide was used to adjust the pH of the preparation.

Table 2. Experimental runs and observed responses for BBD of CLP-BSA NPs

Run	Factor 1	Factor 2	Factor 3	Response 1		Response 2		Response 3		Process Yield (%)
	X_1	X_2	X_3	Particle size (nm)		PDI		Drug loading (%)		
				Actual	Predicted	Actual	Predicted	Actual	Predicted	
1	10	8	24	256 ±4.12	254.32	0.249±0.07	0.247	28.9±6.1	28.67	45±5
2	20	8	16.5	253±8.17	252.89	0.349±0.04	0.345	34.2±8.4	34.32	55±3
3	30	8	9	261±3.19	262.98	0.389±0.01	0.388	37.87±1.7	37.91	61±8
4	20	7	24	257±1.97	254.67	0.378±0.39	0.379	32.87±5.3	33.1	58±9
5	10	9	16.5	248±3.01	250.78	0.198±0.58	0.197	28.7±4.2	28.97	47±5
6	20	8	16.5	252±5.17	251.83	0.278±0.04	0.280	34.89±1.9	34.85	51±6
7	10	8	9	249±3.51	245.45	0.212±0.21	0.215	31.98±5.1	32.12	49±3
8	20	9	9	252±4.23	250.67	0.245±0.08	0.247	30.56±7.2	30.78	50±7
9	20	8	16.5	252±1.56	253.35	0.328±0.26	0.327	37.1±3.5	37.54	52±6
10	20	8	16.5	251±2.13	253.74	0.298±0.29	0.298	32.76±6.4	32.65	54±3
11	20	9	24	253±2.65	254.87	0.431±0.14	0.434	31.4±3.2	31.23	57±2
12	30	7	16.5	263±7.95	262.27	0.489±0.23	0.486	36.18±1.8	36.76	60±4
13	20	7	9	252±6.27	251.90	0.453±0.05	0.452	34.39±5.7	34.78	58±9
14	10	7	16.5	254±2.04	253.65	0.297±0.42	0.298	36.89±6.1	36.34	48±3
15	20	8	16.5	252±6.68	251.86	0.391±0.08	0.392	33.89±9.1	33.12	52±8
16	30	8	24	263±5.46	262.56	0.498±0.17	0.497	35.18±4.2	35.45	56±2
17	30	9	16.5	265±4.32	264.36	0.319±0.02	0.321	39±1.3	39.23	59±6

X_1: Polymer concentration (mg\ml), X_2: pH, X_3: Cross linking time (h)

3.2. Statistical Analysis of Data

3.2.1. Response Surface Model-Box Behnken Design

The Design-Expert software's three-dimensional (3D) response-surface plots are utilized to analyse the pattern of variable interaction. RSM was used as a model here as it helps to optimize the process variables with fewer experiments and provides a more accurate prediction of the response [19]. Table 2 includes the factors along with the variables and responses and Table 3 displays the values for a number of statistical characteristics, including multiple correlation coefficients (R^2), F-values, P-values, coefficients of variation, standard deviation, predicted sums of squares, and mean square values. The response-fittings showed that optimized CLP-BSA NPs with small particle size, small PDI, and high drug loading were obtained at the BSA concentration of 10 mg, pH of 7, and cross-linking period of 16.5 hrs, respectively. ANOVA was used to test the findings of the study for each observed response, which are shown in Table 2. In order to assess the impact of independent factors on the dependent responses, three-dimensional response surface plots and contour plots were combined. Through two- and three-dimensional graphs, they aid in identifying the ideal set of experimental parameters and quantifying the connection between the input parameters and the desired output [18, 19].

In Table 3, the residual value gives information about the difference between the predicted and actual value of the response variable, and the degrees of freedom (DF) deals with the greatest number of logically independent values that can fluctuate in a data sample which is known as the degree of freedom. The total sum of squares (SS) facilitates the expression of the overall variation attributable to several factors. The mean square value (MS) is obtained by dividing the SS and DF value [19] which is used to determine the significance of factors.

3.3. Characterization of Nanoparticles

3.3.1. Drug Polymer Compatibility Study

The drug and polymer compatibility were determined by FTIR spectroscopic studies. The FTIR spectra of CLP, BSA, physical mixture of CLP & BSA and CLP-BSA NPs were recorded and compared (Table 4 & Figure 3). The CLP-BSA NPs spectra showed principal peaks of CLP along with the peaks of BSA, signifying the compatibility of CLP and BSA.

Table 3. Statistical analysis results of particle size, PDI, drug loading

Parameters	DF	SS	MS	F Value	P value	R^2	SD	C.V. %	Adj R^2	Pred R^2
Particle size										
Model	9	414.51	46.06	34.85	<0.0001*	0.9782	1.15	0.4510	0.9782	0.7189
Residual	7	9.25	1.32							
Total	6	423.76								
PDI										
Model	9	0.1254	0.0139	8.73	0.0046 *	0.9182	0.0400	11.71	0.8129	0.5156
Residual	7	0.0112	0.0016							
Total	16	0.1366								
% Drug loading										
Model	9	130.13	14.46	7	0.0089*	0.9001	1.44	4.23	0.7716	0.4373
Residual	7	14.45	2.06							
Total	16	144.58								

* Significant

Table 4. IR interpretation of FTIR spectrum of polymer, drug, physical mixture and optimized NPs

Functional groups	BSA	CLP	Physical mixture BSA & CLP	Optimized CLP-BSA NPs
OH- stretching	3061.82	-	3109.23	3303.20
C=0 stretching ester	1662.38	1752.89	1754.33	1728.47
C-Cl stretch	-	586.21	586.21	586.21
N-H bending	1448.29	-	1573.29	1538.81
Pyridine methylene rock	-	1068.98	1068.98	1073.25
Benzene derivatives	-	712.65	715.53	702.59

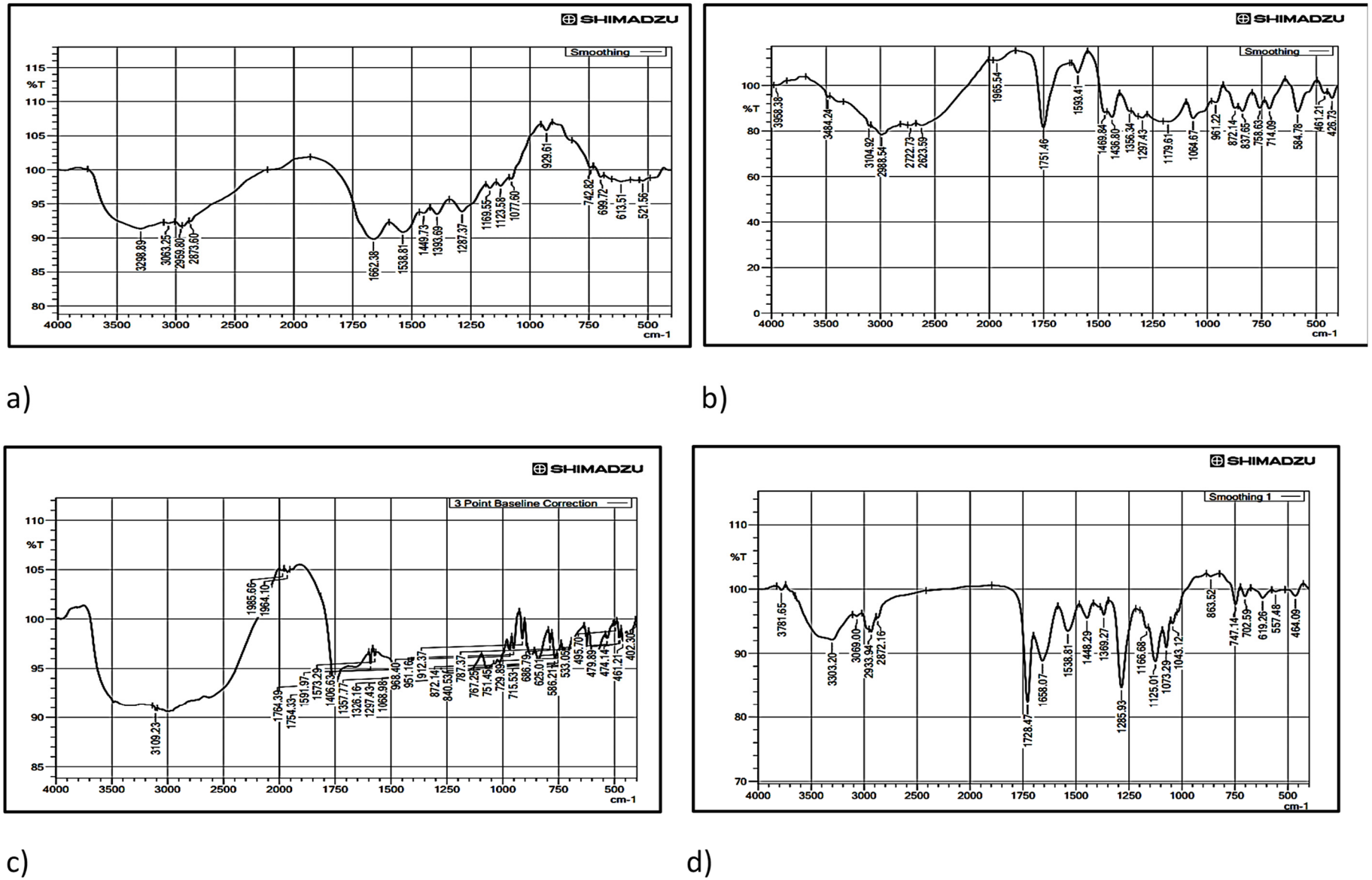

Figure 3. FTIR spectrum of a) BSA, b) CLP, c) Physical mixture of CLP and BSA, d) optimized CLP-BSA NPs

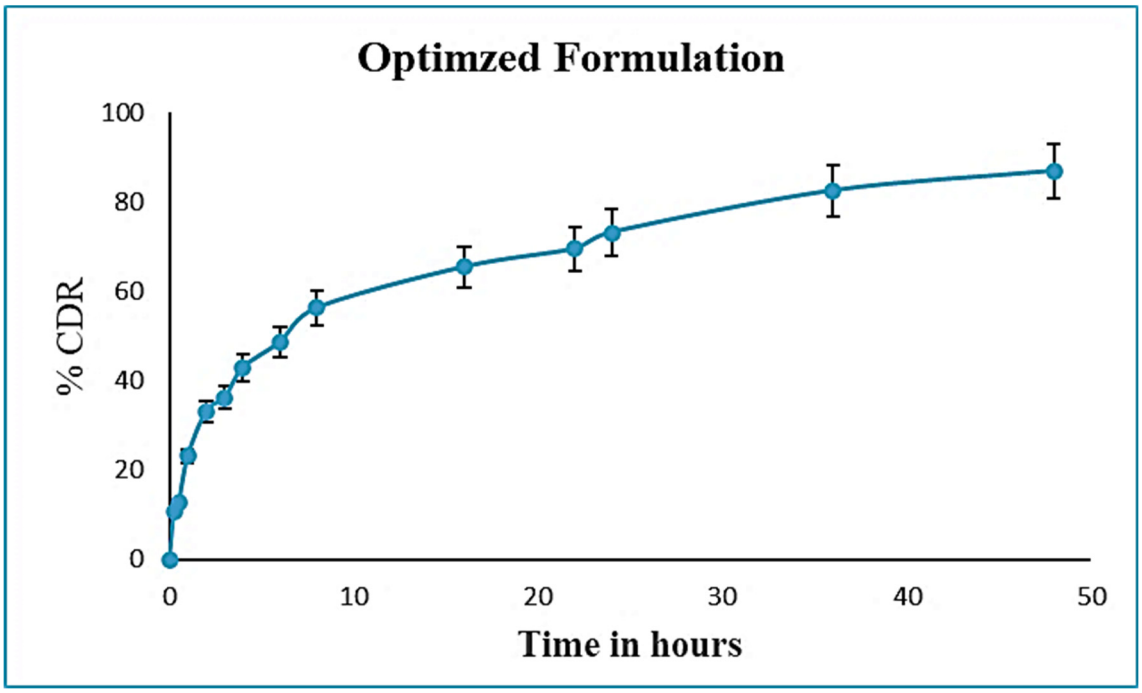

Figure 4. Cumulative drug release profile of optimized CLP-BSA NPs

3.3.2. Process Yield & Drug Loading

The prepared nanoparticles were further processed for characterization parameters like process yield and drug loading. The process yield and drug loading ranged from 45-61% and 28.7-39% respectively (Table 2).

3.3.3. *In vitro* Drug Release Studies

In vitro drug release study was done for all the formulations by suspending the CLP-BSA NPs in pH 7.4 Phosphate buffer solution and cumulative percentage drug release of CLP-BSA NPs was determined up to 48 hrs. The results suggested that the %CDR for 17 formulations at 48 hrs ranged from 48.02 to 86.84%. The % CDR for optimized formulation at 48hrs was 86.84% (Figure 4), and the high % CDR could be due to increased concentration of polymer.

4. Optimization

4.1. Effects on Particle Size of CLP-BSA NPs

The particle size of CLP-BSA NPs was determined by using Malvern Zetasizer Nano-S90 nanoparticle analyser and it ranged from 248 – 265nm (Table 2). Albumin concentration and pH had an impact on the coagulation of albumin molecules and the particle size of nanoparticles. Brownian motion may have provided extremely small particles with enough energy to keep them agitated, preventing the precipitation of nanoparticles and so improving stability [26]. The following polynomial equation explained the effect of factor levels on particle size

$$\text{Particle size} = +252.00 + 5.62A - 1B + 1.7\,C + 2AB - 1.25AC - 1BC + 4.62A^2 + 0.8750B^2 + 0.6250C^2$$

The particle size of nanoparticle increased with the increase in concentration of BSA and cross-linking time (Factor A and C) (Figure 5). The factor A and B showed a positive correlation with Particle size (Figures 6-8).

High BSA concentrations increase the probability of coagulation, as the protein molecules are more likely to interact electrostatically and hydrophobically. The coagulation of the molecules was boosted by larger hydrophobic contacts with BSA, which resulted in bigger particles. As a result, nanoparticles with the desired size range of 100 - 200 nm [27] could be formed with a sufficient BSA concentration. The effect of pH on particle size was greater when combined with BSA concentration because higher pH increases electrostatic repulsion, which reduces the possibilities of coagulation between albumin molecules, which could otherwise lead to the formation of larger particles [28]. ANOVA and polynomial equation data were statistically analysed in the same way. The expected and actual particles are shown and the values are closer together (Figure 9). As a result, the model was significant (Table 3).

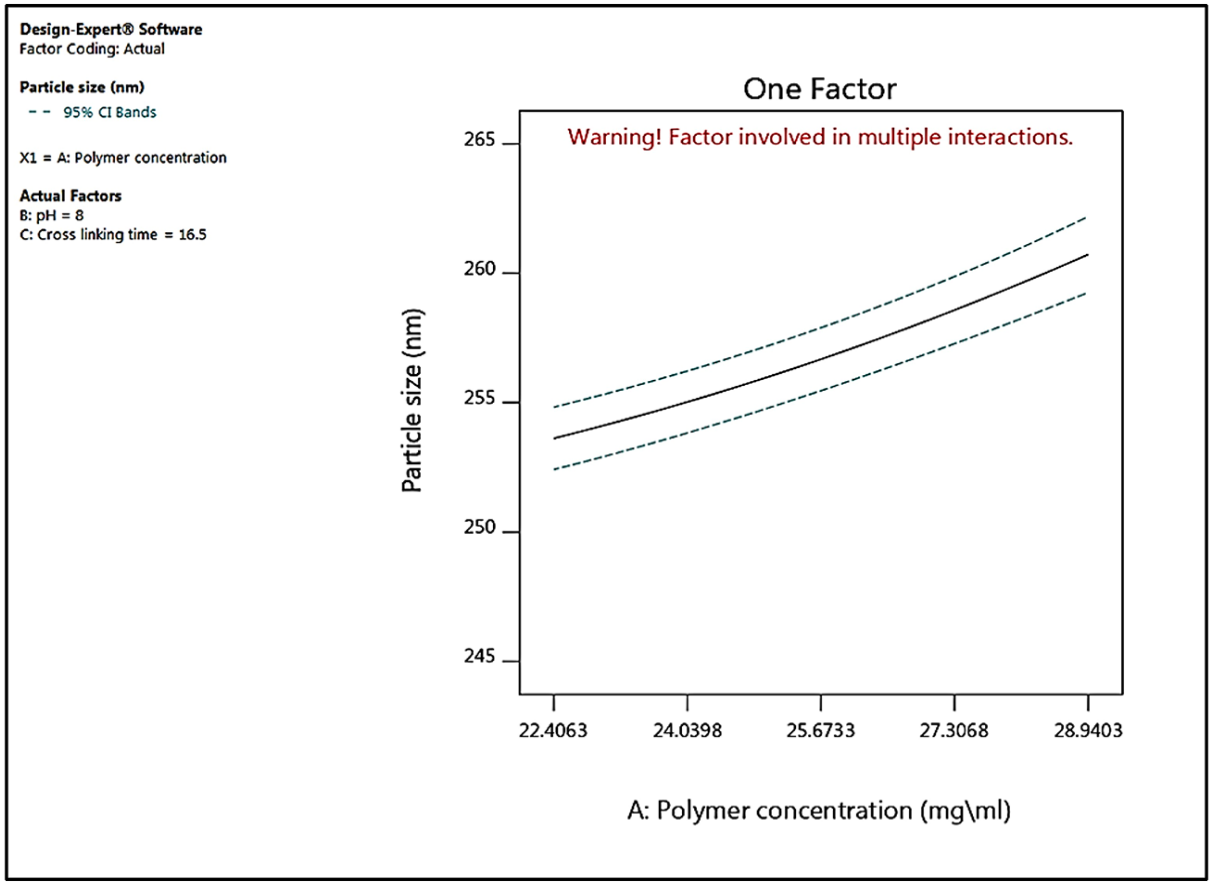

Figure 5. One factor response graph of polymer concentration against Particle size

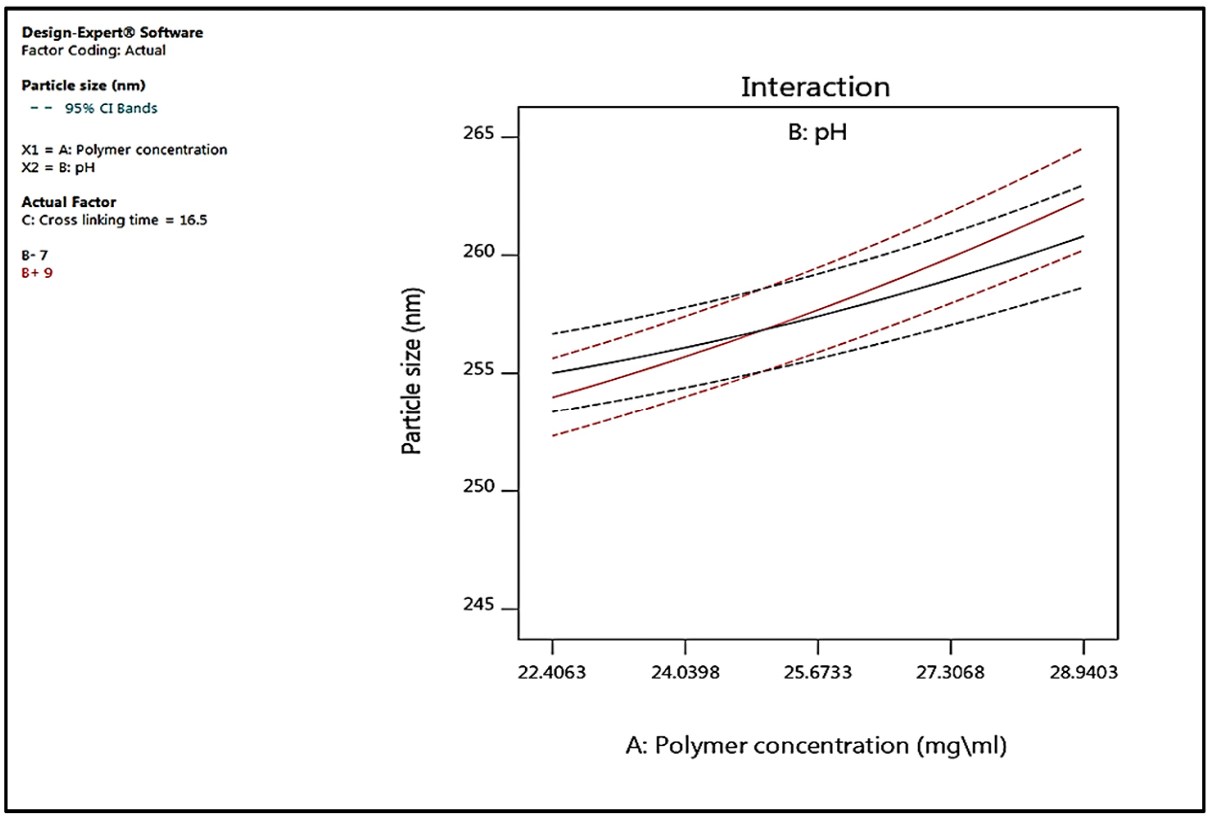

Figure 6. Interaction graph of polymer concentration and pH against Particle size

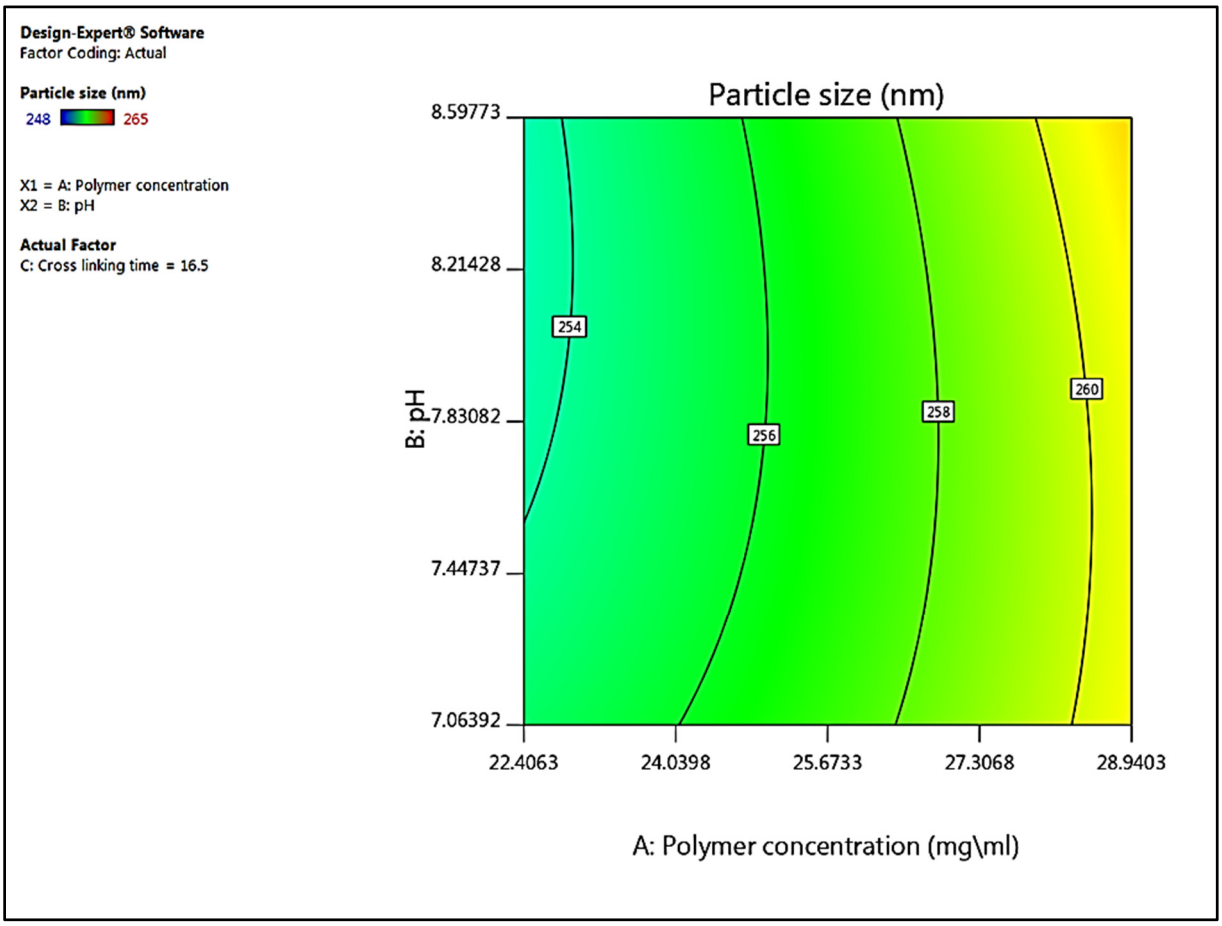

Figure 7. Contour plots of polymer concentration and pH against response Particle size

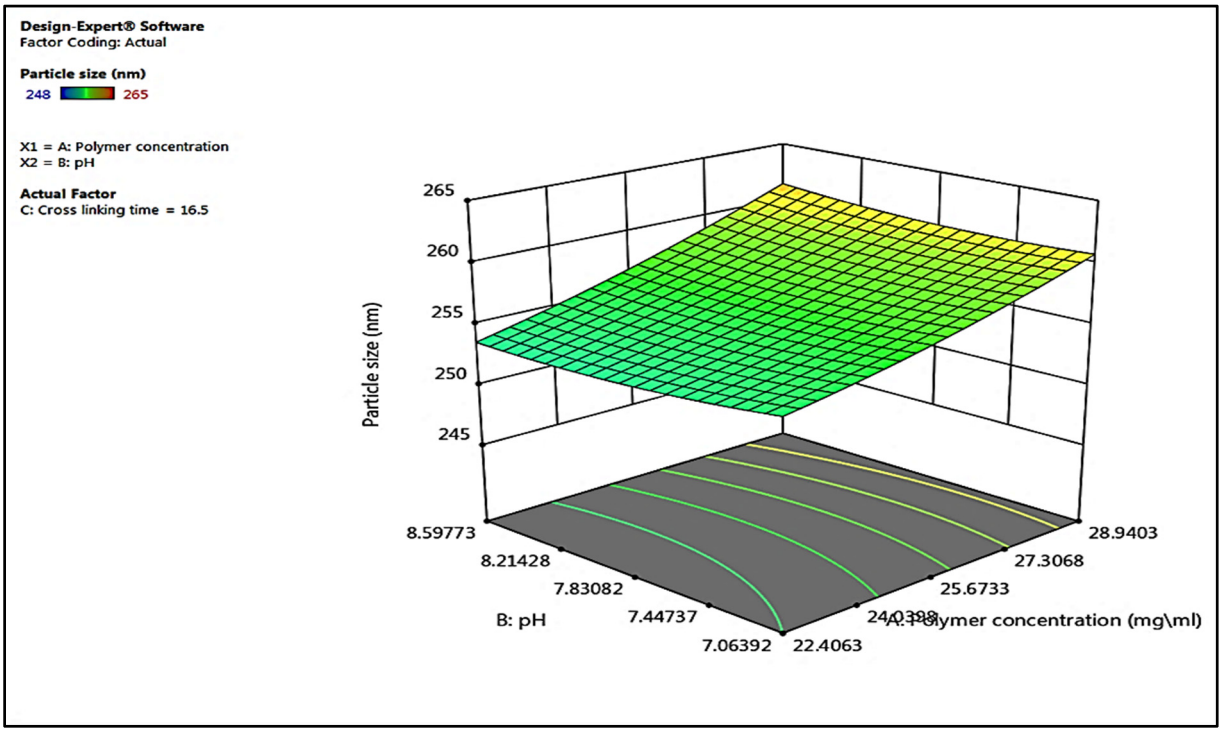

Figure 8. 3D surface plots of polymer concentration and pH against response Particle size

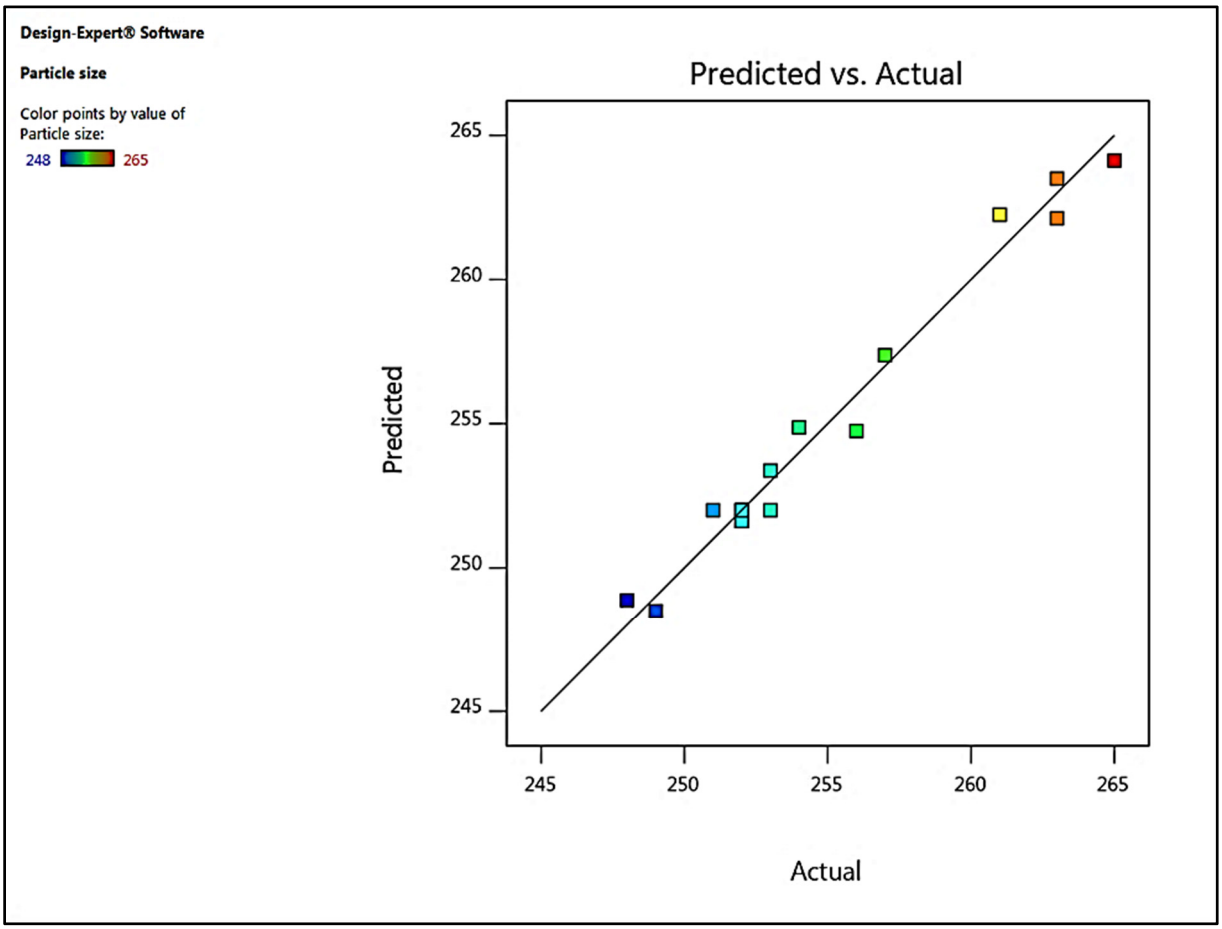

Figure 9. Predicted v/s actual correlation of Particle size

4.2. Effects on PDI of CLP-BSA NPs

The nanoparticles PDI value indicates the stability of the preparation; polydisperse systems have a higher tendency to aggregate than monodispersed systems. A PDI greater than 0.7 indicates a wide particle size distribution, while a PDI less than 0.5 indicates a highly monodispersed system [29].

The PDI of CLP-BSA NPs varied from 0.198 to 0.498 for various factor level combinations as given in Table 2. The independent factors affecting PDI were the concentration of BSA, pH and cross-linking time. The responses obtained were denoted by the following quadratic equation:

$$PDI = + 0.3288 + 0.0924\ A - 0.0530\ B + 0.0321\ C - 0.0177\ AB + 0.0180\ AC + 0.0653\ BC - 0.0214\ A^2 + 0.0183B^2 + 0.0296C^2$$

The PDI depended mainly on the concentration of BSA. According to the response surface and contour plots, when factor A increased, the PDI likewise increased (Figure 10). This is because when the polymer concentration increases, so does the polymeric contact, which enhances the coagulation of the formed nanoparticles. The influence of pH and cross-linking duration on CLP- BSA NPs was minimal, but when BSA concentration and pH increases (Figures 11-13), PDI reduces because the protein-protein interaction decreases at alkaline pH, which is distant from the isoelectric pH of BSA, resulting in decreased coagulation of particles. Figure 14 and Table 3 specify that the actual and predicted values were located close to each other indicating the significance of the model.

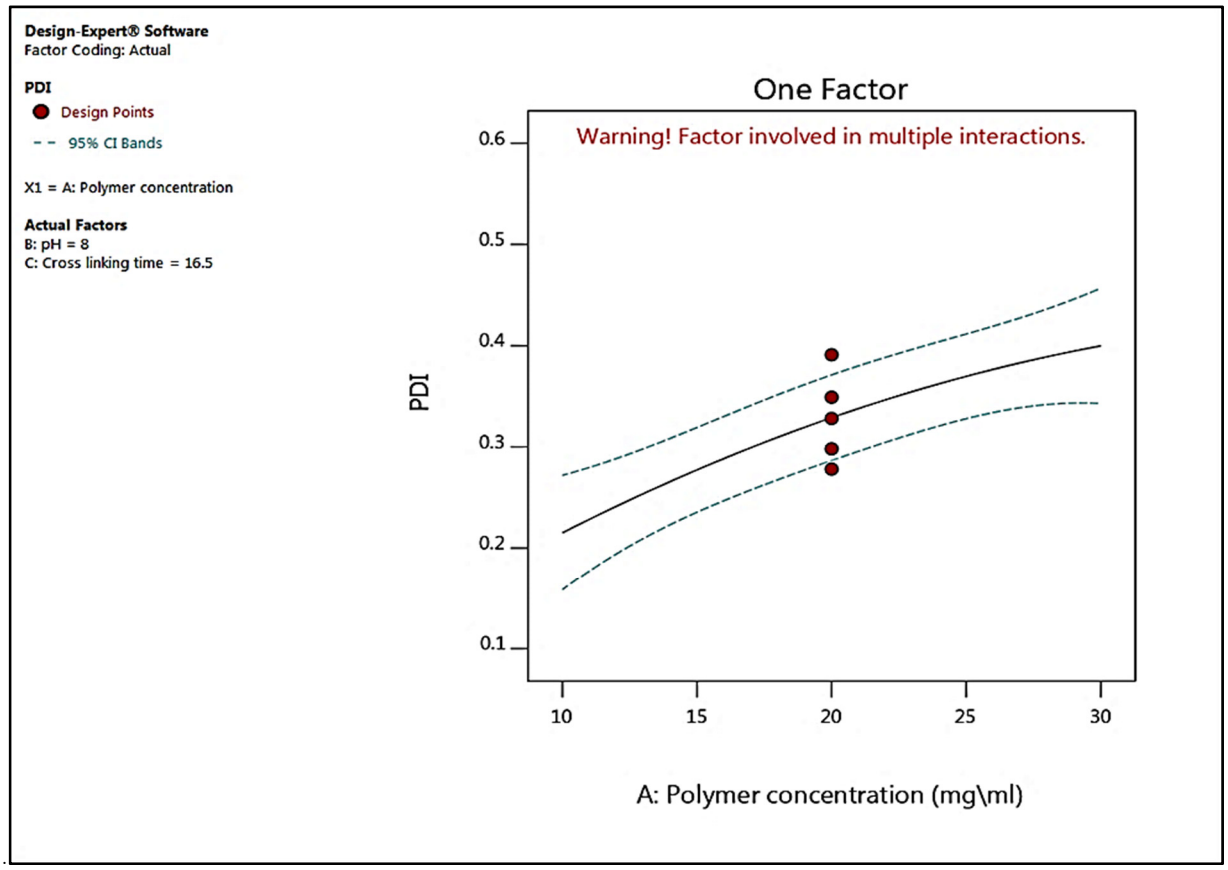

Figure 10. One factor response graph of polymer concentration against PDI

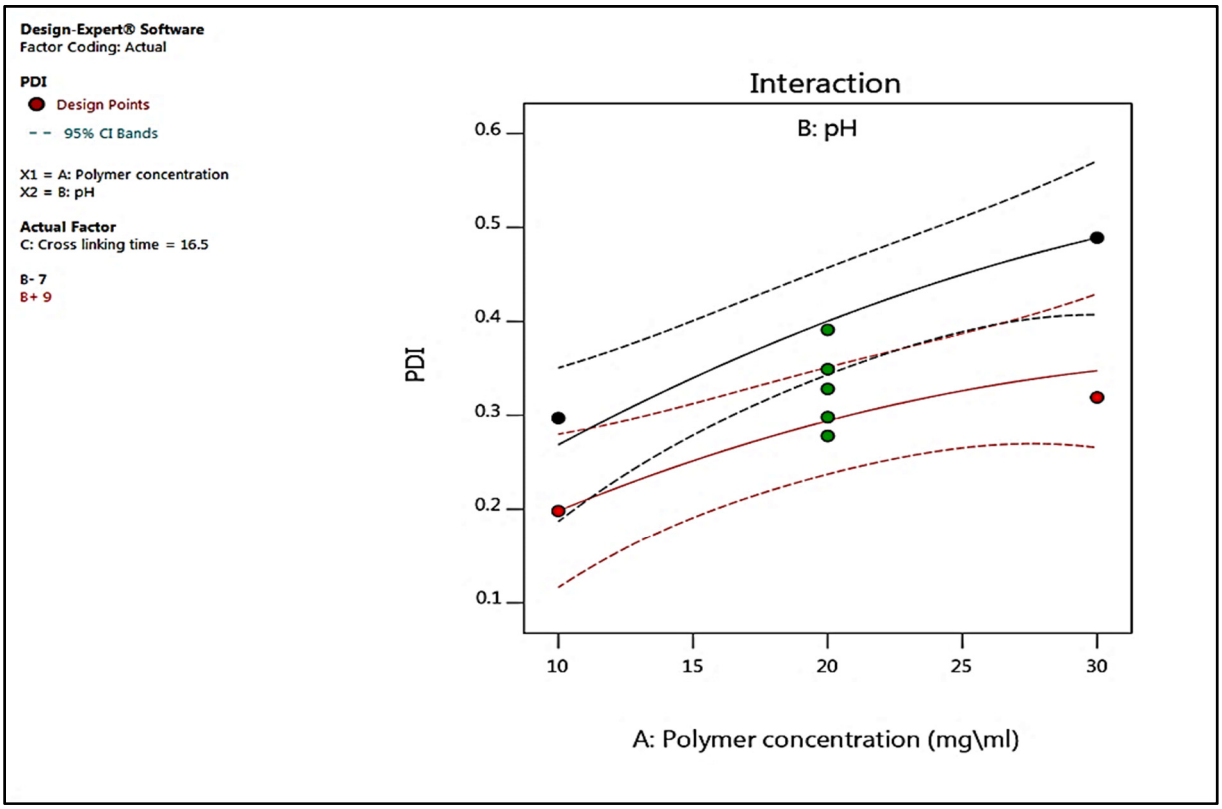

Figure 11. Interaction response graph of polymer concentration and pH against PDI

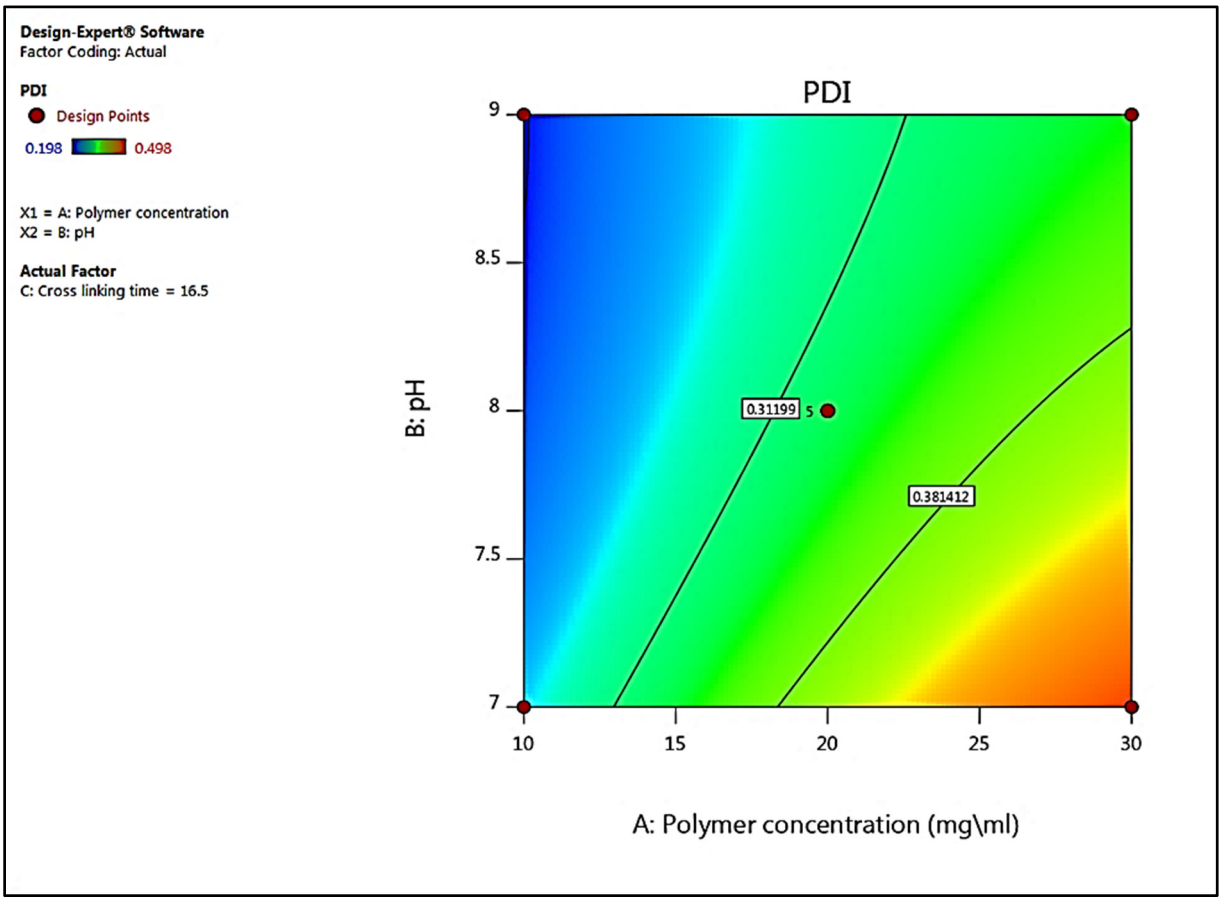

Figure 12. Contour plots of polymer concentration and pH against response PDI

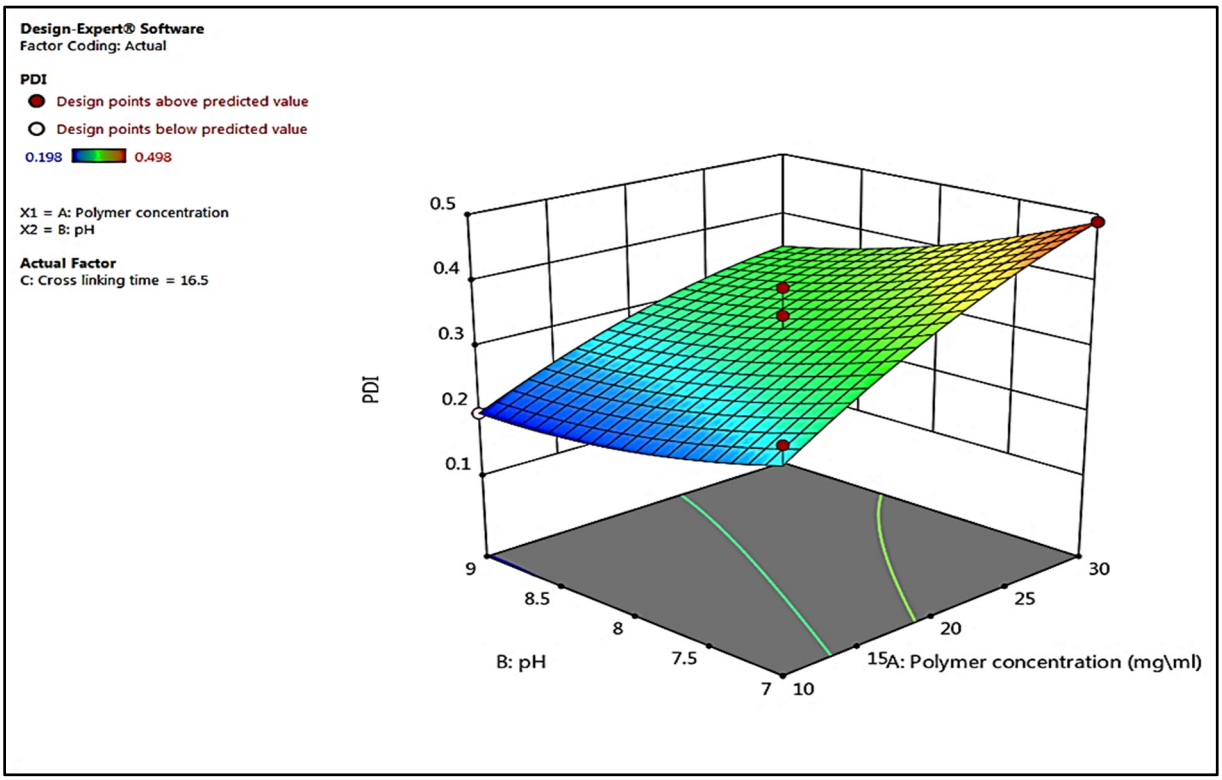

Figure 13. 3D surface plots of polymer concentration and pH against response PDI

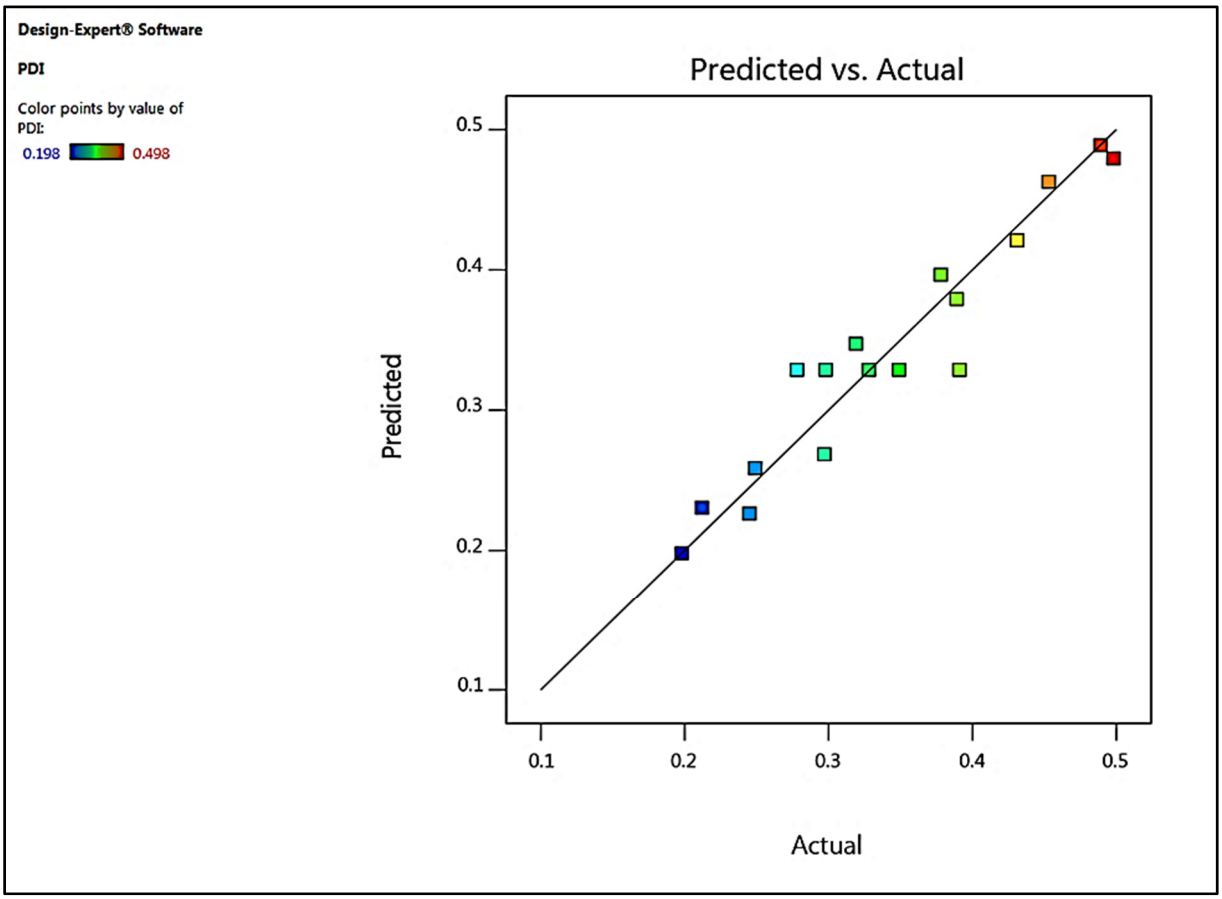

Figure 14. Predicted v/s actual correlation of PDI

4.3. Effects on Drug Loading of CLP-BSA NPs

The % drug loading (DL) of nanoparticles ranged from 28.7% to 39% is given in Table 2. The drug loading capacity might be due to the presence of multiple binding sites in the protein molecules of the polymer and the drug loading mechanism could be due to hydrophobic interactions, electrostatic attraction, and covalent bonding [29]. The impact of factors on drug loading is described by the following polynomial equation.

$$\% DL = + 34.57 + 2.72\ A + 1.33\ B - 0.8063\ C + 2.75\ AB + 0.0975\ AC + 0.59BC - 0.9010A^2 - 0.2765\ B^2 - 1.99\ C^2$$

Figures 15-18 showed the response surface and contour plots for % DL. The % DL increased as the concentration of BSA increased, which could be due to improved drug adsorption or interaction with the polymer at high polymer concentrations. The formulation's cross-linking time has a negative impact on the % DL of CLP. Longer cross-linking times could result in medication leakage from the polymeric matrix. The drug loading was enhanced as the pH increased to 9, and it could be due to increased BSA solubility at basic pH. It was observed from Figure 19 and Table 3 that the predicted and actual %DL data were close to each other giving the significant results.

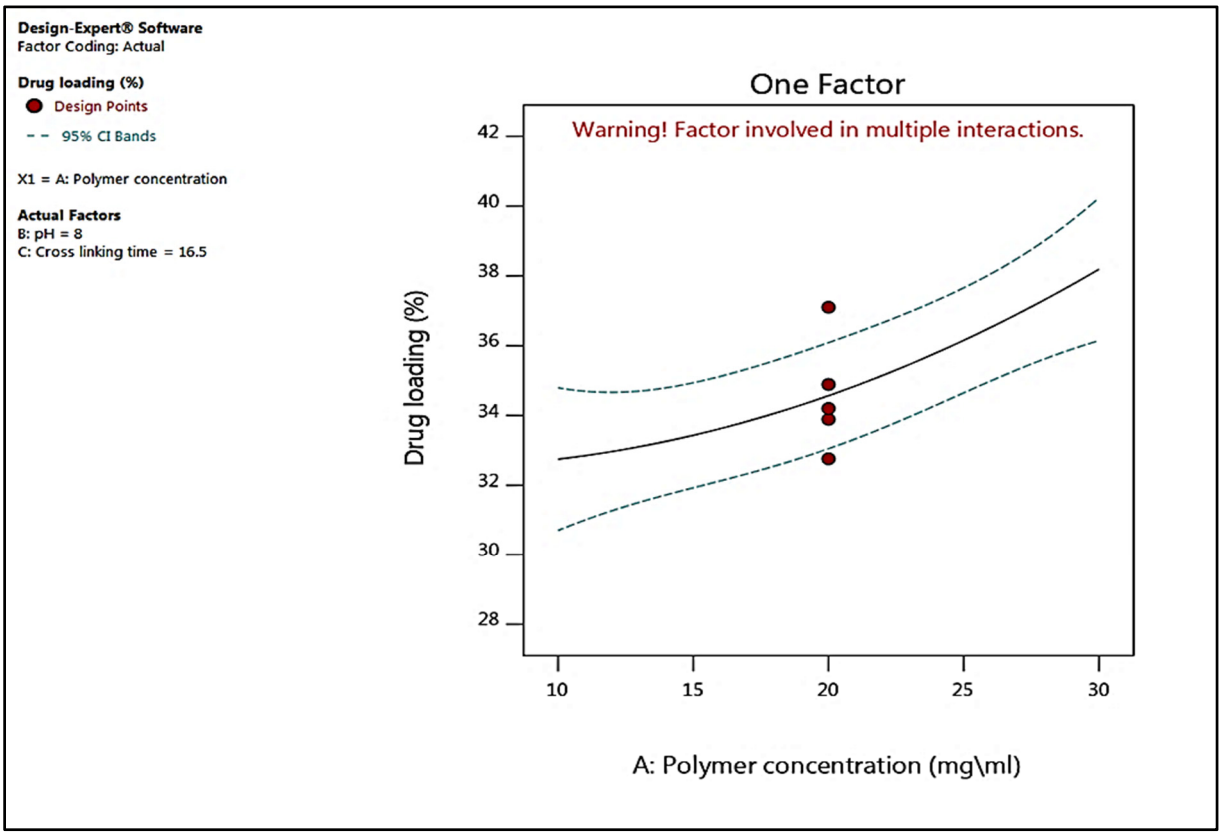

Figure 15. One factor response graph of polymer concentration against drug loading

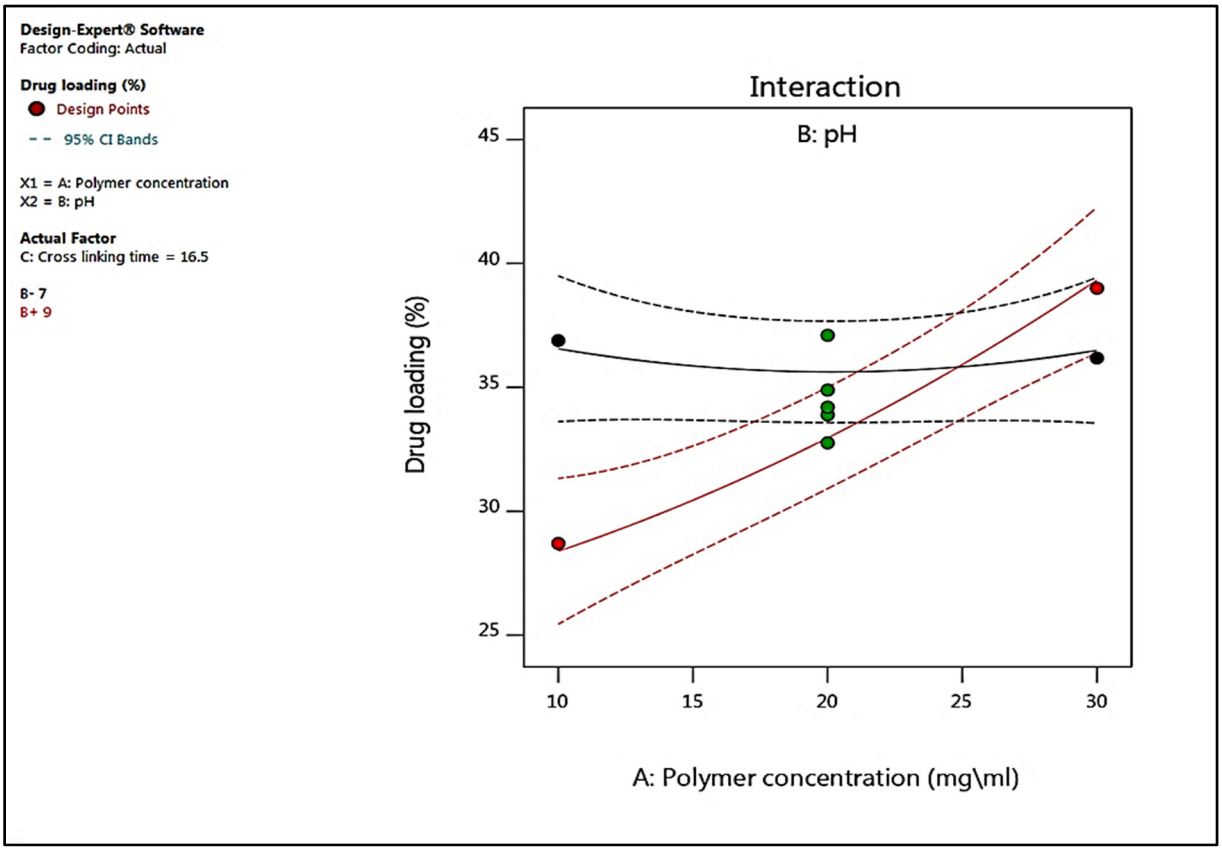

Figure 16. Interaction response graph of polymer concentration and pH against drug loading

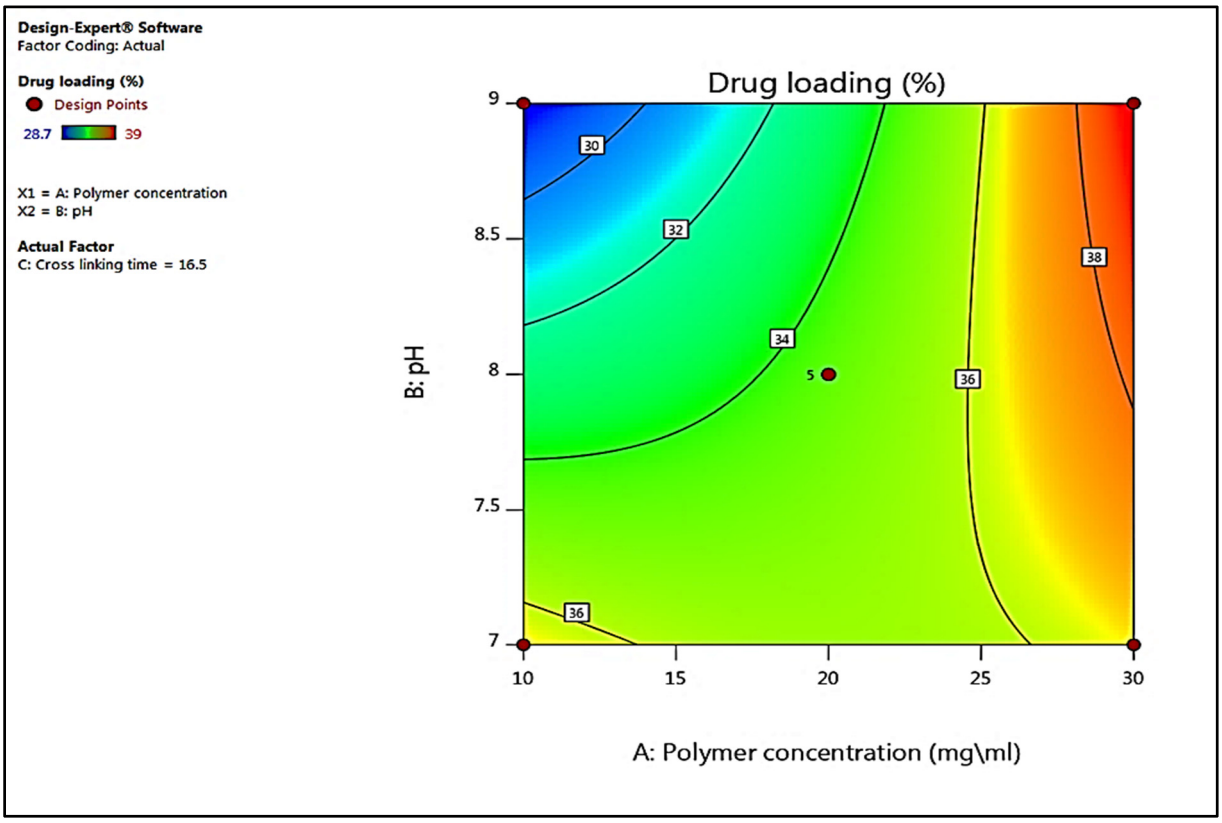

Figure 17. Counter plot polymer concentration and pH against response drug loading

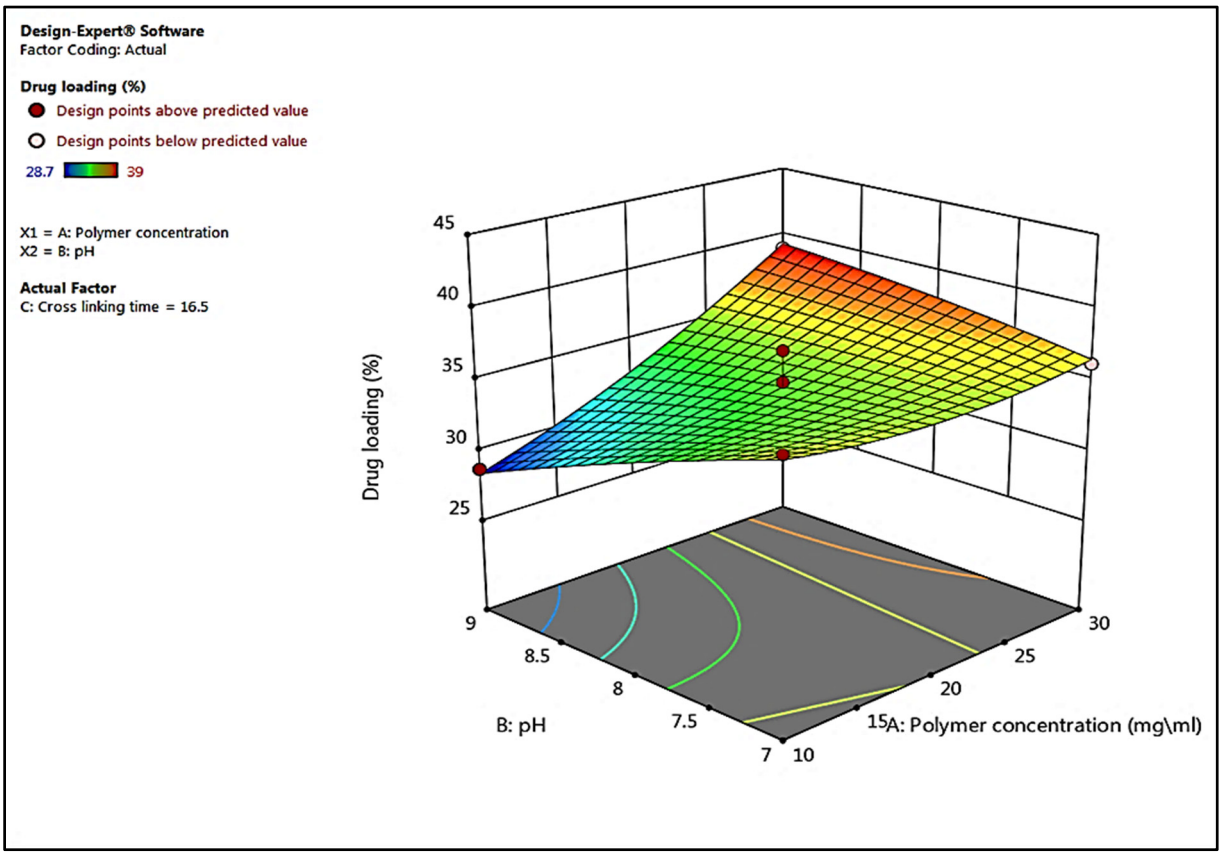

Figure 18. 3D surface plots of polymer concentration and pH against response drug loading

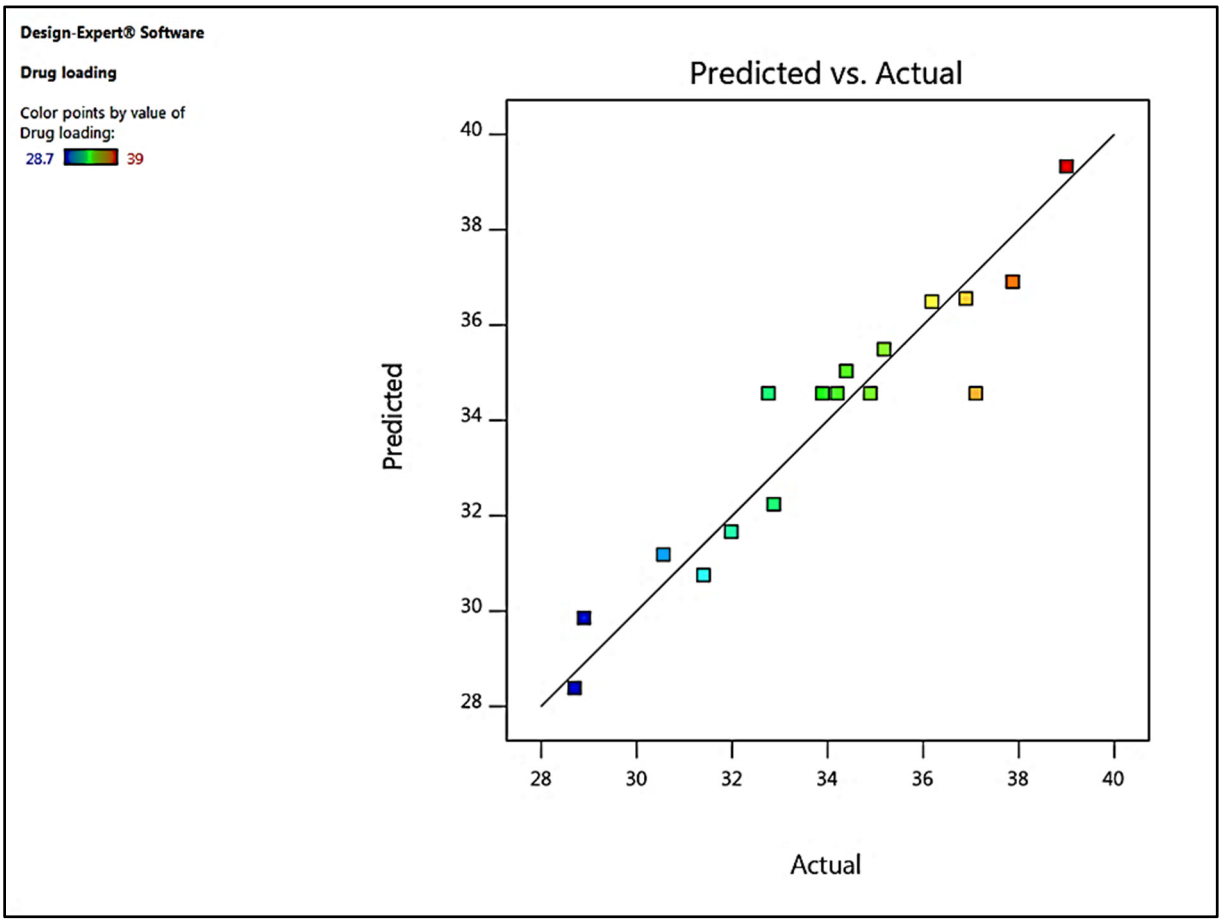

Figure 19. Predicted v/s actual correlation of drug loading

5. Evaluation of Optimized Formulation

5.1. Determination of Zeta Potential

The effective electric charge on the surface of a nanoparticle is measured by its zeta potential. By monitoring the mobility of nanoparticles in an applied electric field, the zeta potential of nanoparticle suspension was measured. The zeta potential was conducted at a temperature of 25°C and a measurement angle of 90°. The zeta potential value of the optimized formulation of CLP-BSA NPs was found to be -27 mV (Figure 20). The value clearly indicates that the formulated nanoparticles were stable [30].

5.2. TEM Analysis

The morphological characteristics of CLP-BSA NPs were characterized by TEM. The TEM pictures (Figure 21), depicted the particles' spherical shape and smooth surface area. The images (Figures 21 & 22), also demonstrated the homogeneous distribution of nanoparticles.

Calculation Results

Peak No.	Zeta Potential	Electrophoretic Mobility
1	-27 mV	0.000008 cm2/Vs
2	--- mV	--- cm2/Vs
3	--- mV	--- cm2/Vs

Zeta Potential (Mean) : -27 mV
Electrophoretic Mobility Mean : 0.000008 cm²/Vs

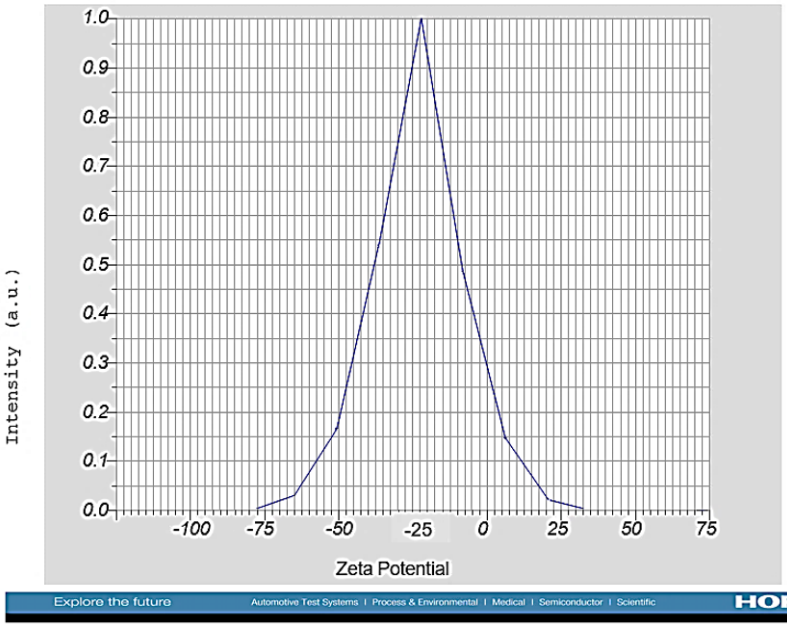

Figure 20. Zeta potential of optimized CLP-BSA NPs

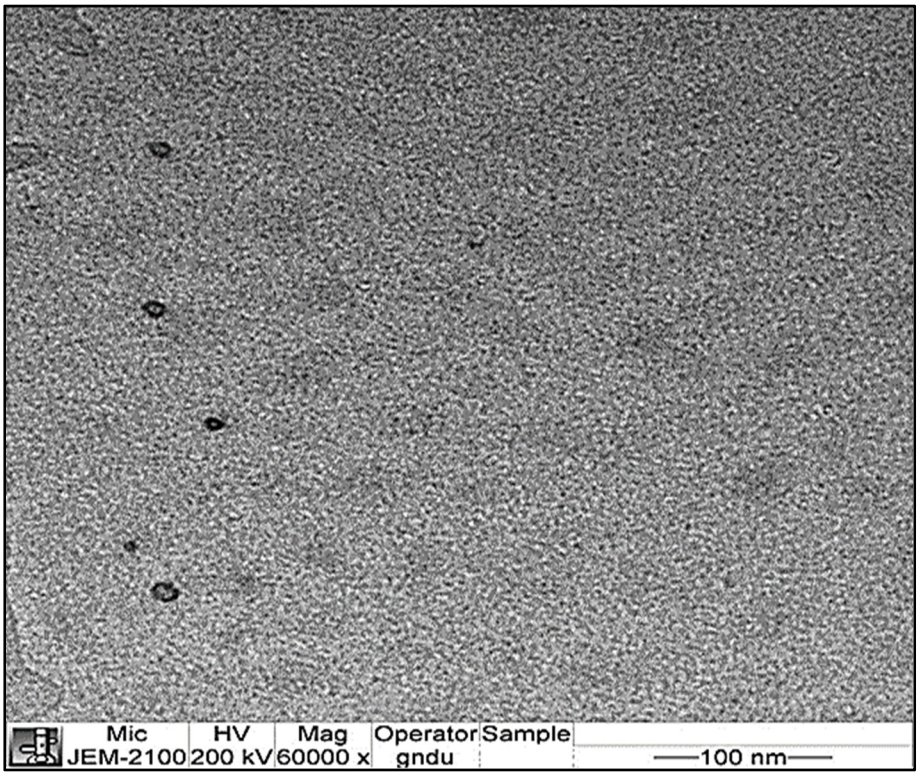

Figure 21. TEM images of optimized CLP-BSA NPs

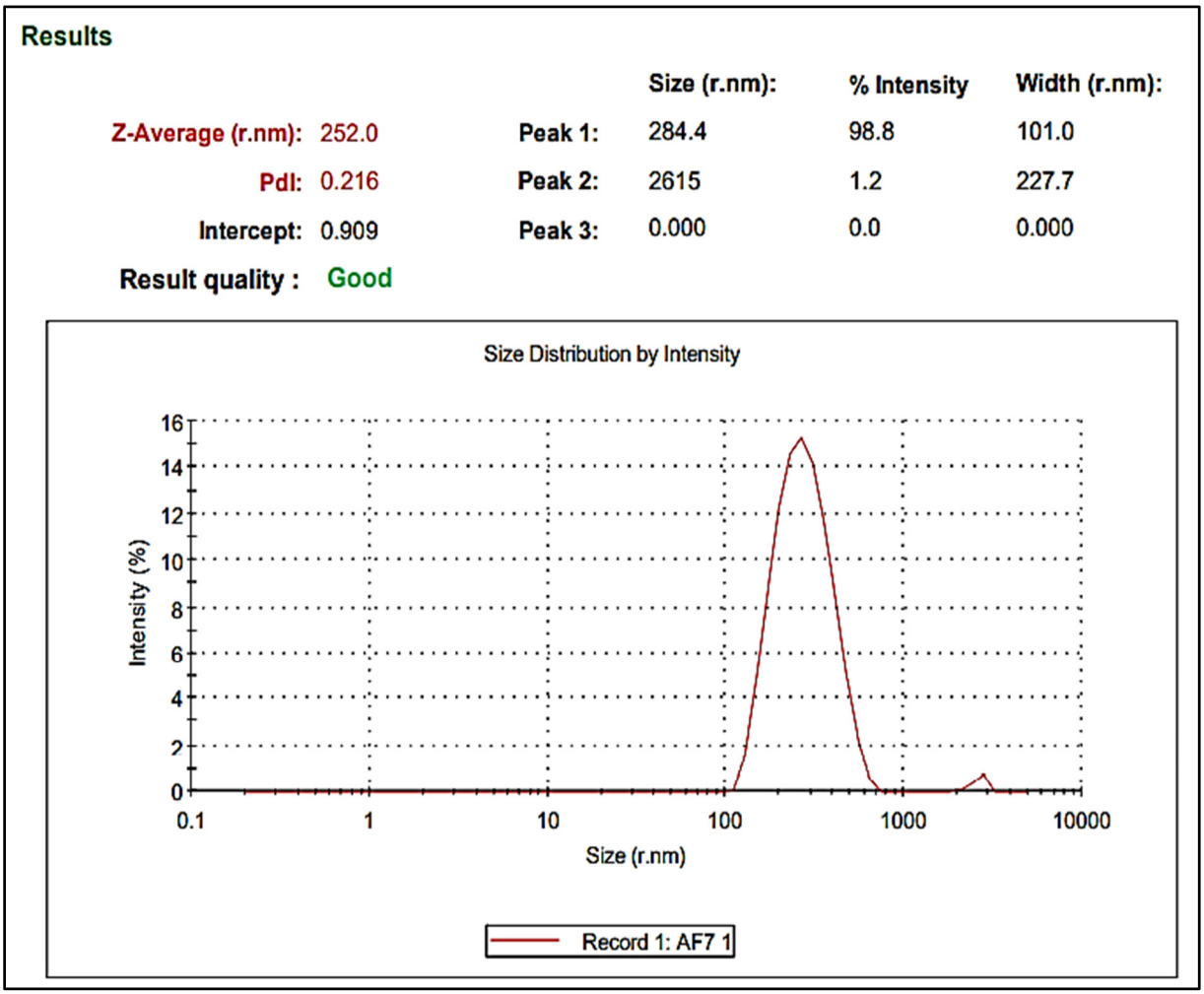

Figure 22. Particle size analysis of optimized CLP-BSA NPs

5.3. Differential Scanning Calorimetry

The differential thermograms for CLP and CLP-BSA NPs were obtained and evaluated (Figures 23 & 24). The thermogram of CLP depicted an endothermic change with a peak at 185.97°C which was closely related to its melting point of 184°C [31]. The CLP-BSA NPs did not show any peak corresponding to CLP. This led to the conclusion that CLP was in an amorphous or disordered crystalline state in nanoparticles, which prevented crystal formation and increased formulation stability.

5.4. Drug Release Kinetics

The release data obtained from the %CDR was fitted to various kinetic models to obtain the release constant and regression coefficient (Figure 25). The highest regression coefficient value was obtained for the Higuchi model, indicating the diffusion-controlled type release of drug [32, 33]. For all of the formulations, the n value of the Korsmeyer-Peppas model was less than 0.45, indicating a Fickian type of drug release mechanism.

Table 5 illustrated the optimum combinations of parameters selected for the optimized formulations by comparing with the initial and predicted values. The optimized formulation was prepared in the triplicate manner through the optimal levels of the independent variables and was subjected to animal studies to determine their efficacy.

5.5. Animal Studies

The effectiveness of prepared CLP-BSA NPs was confirmed by checking their effect on bleeding and clotting time in Wister albino rats. As shown in Figures 26, 27 & 28, and Table 6, the bleeding and clotting time of the group treated with CLP-BSA NPs was found to be pronged as compared to the inference of groups that were treated with an equivalent dose of free drug and 0.9% NaCl solution (control).

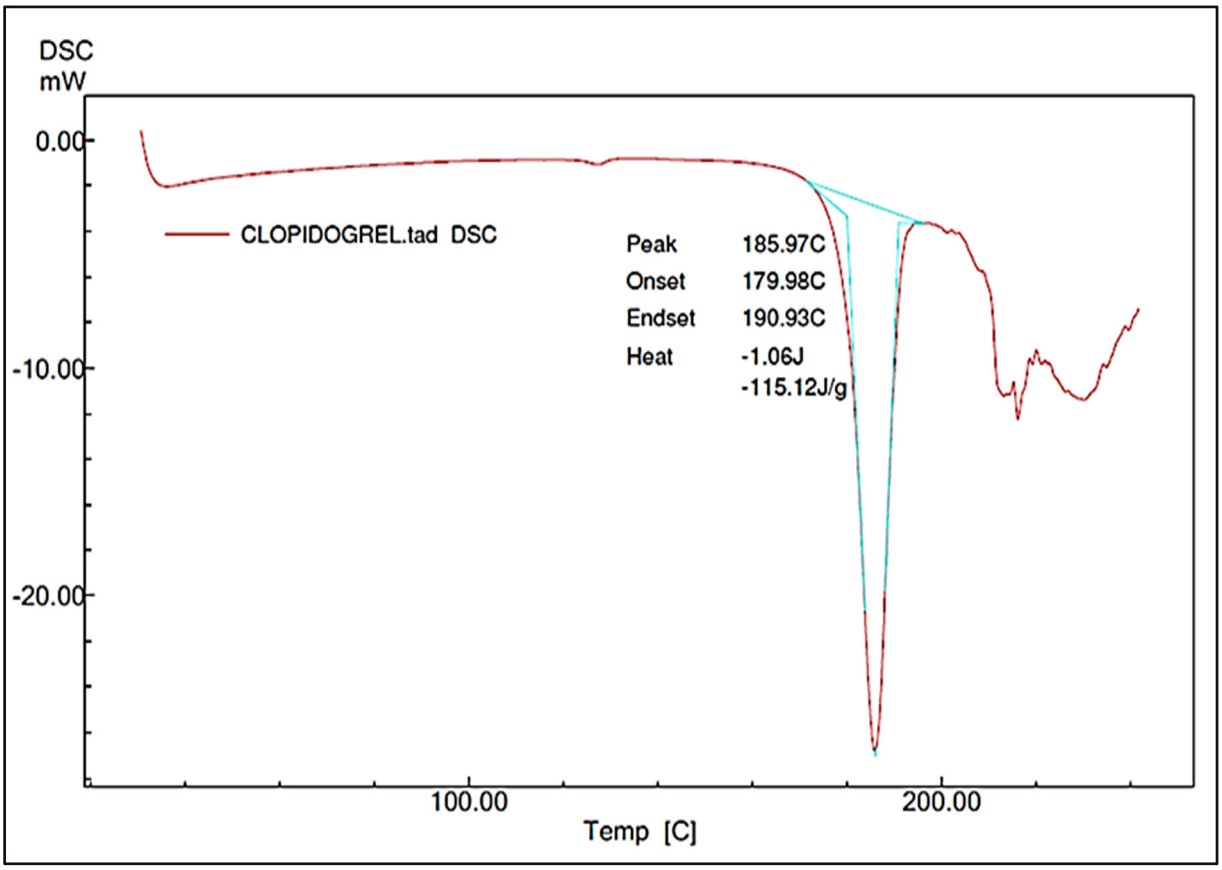

Figure 23. Thermogram of CLP

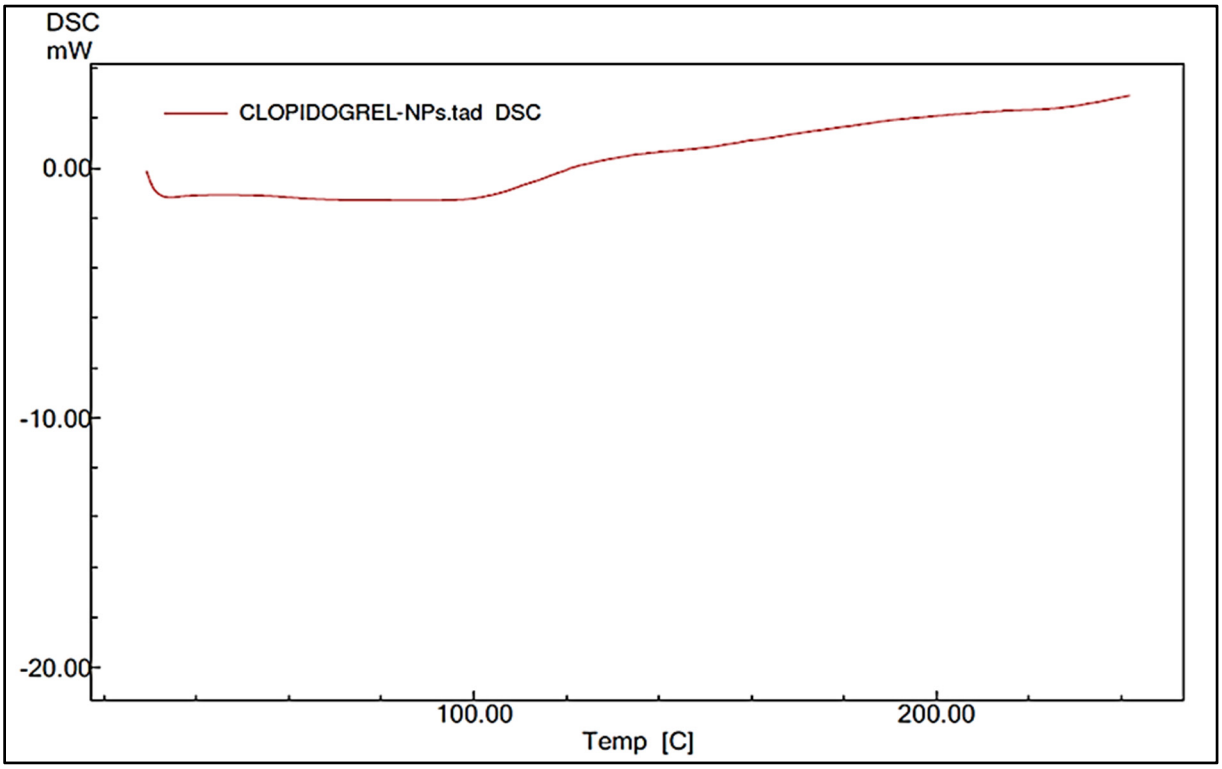

Figure 24. Thermogram of CLP-BSA NPs

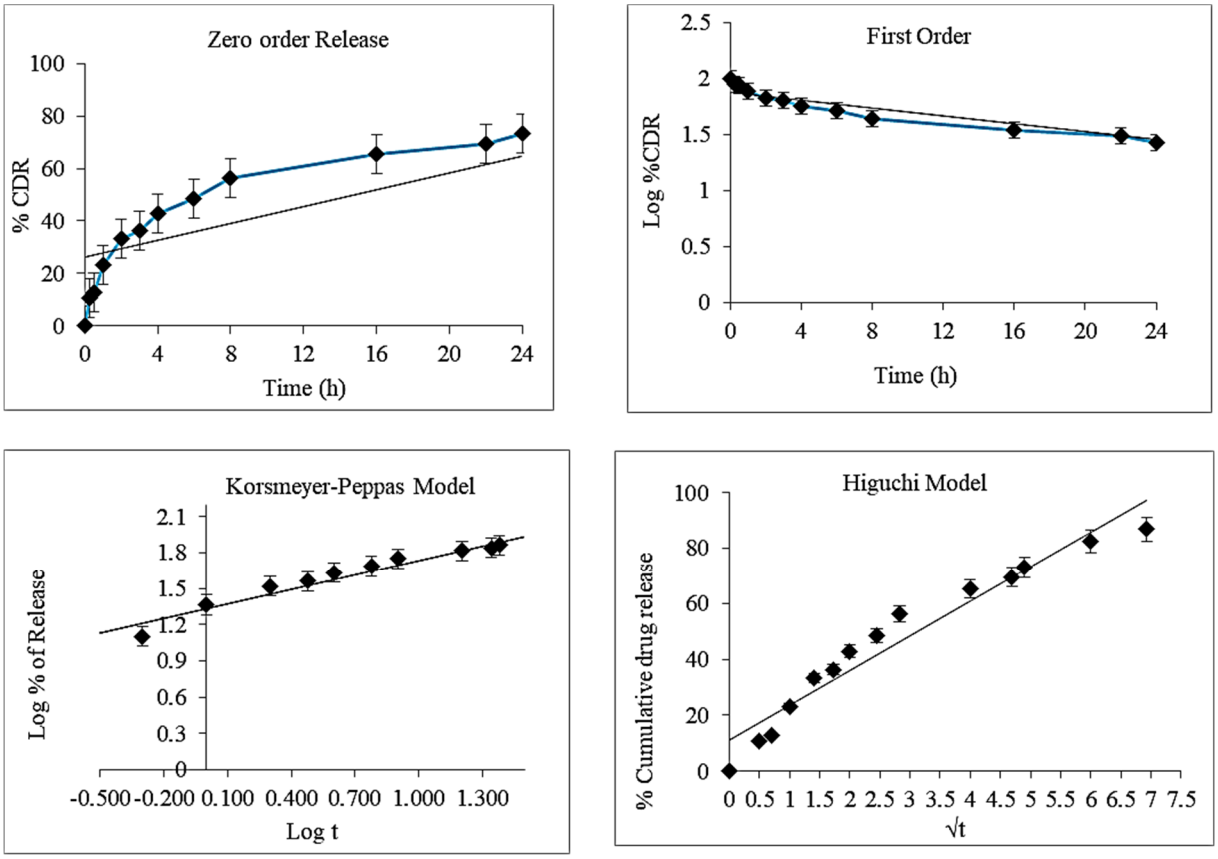

Figure 25. Drug release kinetics profile of optimized CLP-BSA NPs

Table 5. Optimum combinations of parameters by comparing with the initial and predicted values

Formulation	Values	Response	Predicted	Actual	Std. Dev	SE Mean
Polymer concentration (mg)	10	Particle size	254.875	252	1.1495	0.9955
pH	7	PDI	0.2686	0.216	0.0399	0.03461
Cross linking time (h)	16.5	Drug loading	36.55	34.98	1.4367	1.2442

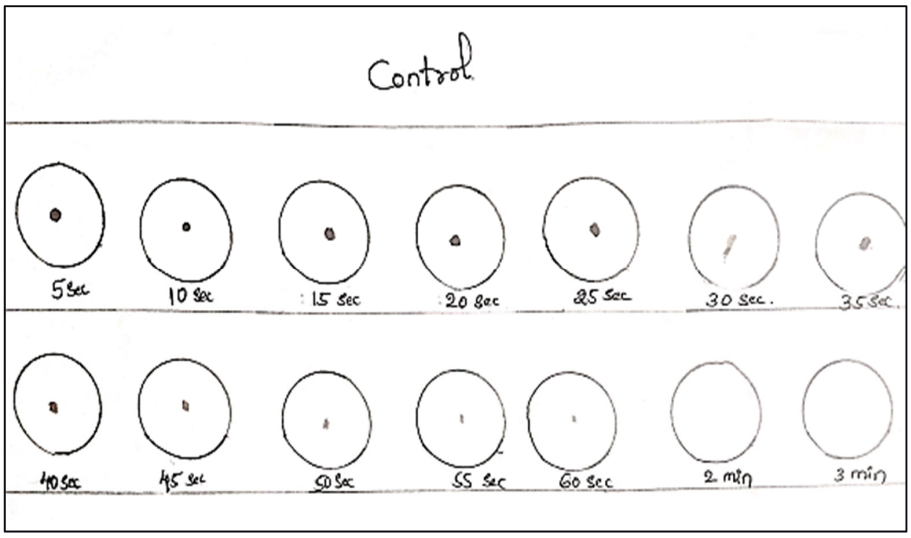

Figure 26. Bleeding time records of control

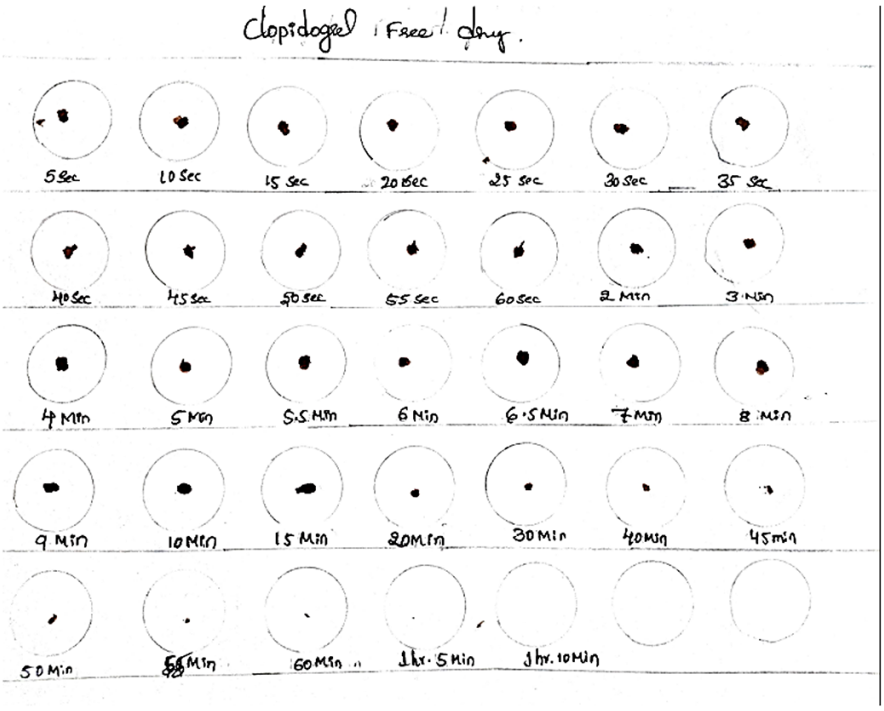

Figure 27. Bleeding time records of free drug (CLP)

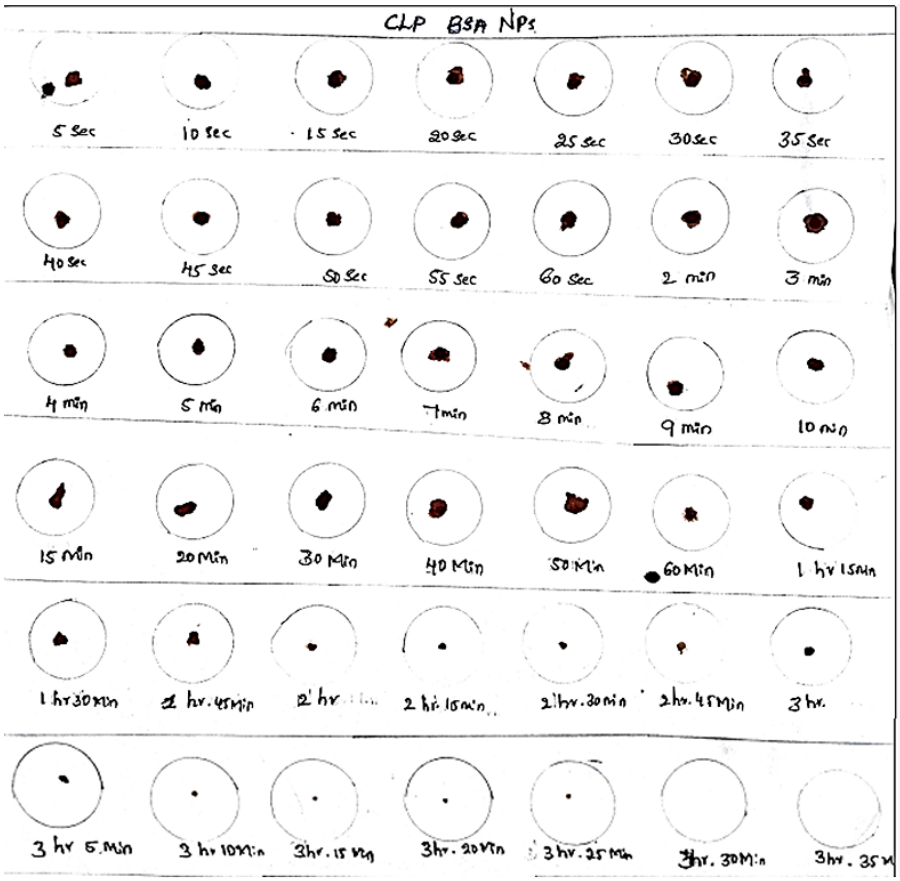

Figure 28. Bleeding time records of CLP-BSA NPs

Table 6. Report of clotting time

Sl.No	Groups	Average clotting time
1	Control	45 ± 7 sec.
2	Free CLP drug	2 min 26 sec ± 0 min 15 sec.
3	CLP-BSA NPs	3 min 50 sec ± 1 min 23 sec.

6. Conclusions

In the present study, an attempt was made to formulate a nanoparticle drug delivery system for clopidogrel drug containing BSA as a polymer. The drug polymer compatibility studies of selected drug and polymer were carried out by FT-IR spectroscopy. The compatibility study showed that there was no possible interaction between the selected drug and the polymer. CLP-BSA NPs were prepared by desolvation technique. The CLP-BSA NPs preparation procedure was optimized by using Box-Behnken design for independent variables such as polymer concentration, pH of BSA solution, and Cross-linking time and their effect was checked on particle size, PDI and drug loading. The optimized nanoparticles had a mean diameter of 252 nm, PDI of 0.216, and drug loading of 34.98%. Particle size analysis revealed that the formulated nanoparticles were in nano range and possessed a negative surface charge. The *in vitro* drug release profile of all formulations showed sustained release of drug for 48h. The release kinetics data showed that CLP release from nanoparticles was diffusion controlled and the n values of the Korsmeyer-Peppas model indicate the release mechanism which was Fickian mediated release. Based on this observation, it can be concluded that the formulated nanoparticle drug delivery system containing CLP is safe and produces sustained release of drug for 48h. Further effect was confirmed by checking clotting and bleeding time in Wister albino rats and was found to be prolonged in case of animals treated with CLP-BSA NPs as compared to the free drug and control-treated groups. Overall, it can be concluded that the prepared nanoparticles could be an efficient platform for the management of atherosclerosis.

REFERENCES

[1] Cardiovascular diseases, Who.int, https://www.who.int/india/health-topics/cardiovascular-diseases (accessed on Jan. 1, 2023)

[2] Stary HC, Composition and classification of human atherosclerotic lesions, *Virchows Arch Pathol Anat Histopathol.* Vol. 421, no. 4, pp 277–90, 1992, DOI: https://doi.org/10.1007/bf01660974

[3] India State-Level Disease Burden Initiative CVD Collaborators. The changing patterns of cardiovascular diseases and their risk factors in the states of India: the Global Burden of Disease Study 1990-2016, *Lancet Glob Health*, vol. 6, no. 12, pp. e1339-e1351, 2018, DOI: https://doi.org/10.1016/S2214-109X(18)30407-8

[4] Tegos TJ, Kalodiki E, Sabetai MM, Nicolaides AN, The genesis of atherosclerosis and risk factors: a review, *Angiology*, vol. 52, no. 2, pp. 89-98, 2001, DOI: https://doi.org/10.1177/000331970105200201

[5] Atherosclerosis, News-medical.net, https://www.news-medical.net/health/Atherosclerosis.aspx (accessed on Jan. 10, 2023)

[6] Rafieian-Kopaei M, Setorki M, Doudi M, Baradaran A, Nasri H, Atherosclerosis: process, indicators, risk factors and new hopes, *International Journal of Preventive Medicine,* vol. 5, no. 8, pp. 927-946, 2014, URL: https://www.ncbi.nlm.nih.gov/pmc/articles/PMC4258672/

[7] Smith EB, Transport, interactions and retention of plasma proteins in the intima: the barrier function of the internal elastic lamina, *European Heart Journal,* vol. 11, pp. 72-81, 1990. DOI: https://doi.org/10.1093/eurheartj/11.suppl_e.72

[8] Sangkuhl K, Klein TE, Altman RB, Clopidogrel pathway. *Pharmacogenet Genomics*, vol. 20, no. 7, pp. 463-465, 2010, DOI: https://doi.org/10.1097/fpc.0b013e3283385420

[9] Qureshi M J, Phin F F, Patro S, Enhanced solubility and dissolution rate of clopidogrel by nanosuspension: Formulation via high pressure homogenization technique and optimization using box Behnken design response surface methodology, *Journal of Applied Pharmaceutical Science*, vol. 7, no. 2, pp. 106-113, 2017, DOI: https://doi.org/10.7324/JAPS.2017.70213

[10] Plosker GL, Lyseng-Williamson KA, Clopidogrel: A Review of its Use in the Prevention of Thrombosis, *Drugs*, vol. 67, no. 4, pp. 613-646, 2007, DOI: https://doi.org/10.2165/00003495-200767040-00013.

[11] Esim O, Gedik ME, Dogan AL, Gunaydin G, Hascicek C, Development of carboplatin loaded bovine serum albumin nanoparticles and evaluation of its effect on an ovarian cancer cell line, *Journal of Drug Delivery Science and Technology,* vol. 64, no. 102655, 2021, DOI: https://doi.org/10.1016/j.jddst.2021.102655

[12] Yan S, Zhang H, Piao J, Chen Y, Gao S, et a, Studies on the Preparation, Characterization and Intracellular Kinetics of JD27-loaded Human Serum Albumin Nanoparticles, *Procedia Engineering*, vol. 102, pp, 590-601, 2015, DOI: https://doi.org/10.1016/j.proeng.2015.01.133

[13] Jahanban-Esfahlan A, Dastmalchi S, Davaran S, A simple improved desolvation method for the rapid preparation of albumin nanoparticles, *International Journal of Biological Macromolecules*, vol. 91, pp. 703-709, 2016, DOI: https://doi.org/10.1016/j.ijbiomac.2016.05.032

[14] Boddupalli BM, Ramani R, Anisetti B, Pamujula NH, Development and In-Vitro Anticancer Evaluation of Dual Loaded Nanoparticles on Human Glioblastoma Multiforme Cell line T98G, *Saudi Journal of Biomedical Research,* pp. 88–95, 2019, DOI: https://doi.org/10.21276/sjbr.2019.4.3.2

[15] Li J, Deng J, Yuan J, et al, Zonisamide-loaded triblock copolymer nanomicelles as a novel drug delivery system for the treatment of acute spinal cord injury, *International Journal of Nanomedicine*, vol. 12, pp. 2443-2456, 2017, DOI: https://doi.org/10.2147/IJN.S128705

[16] Humbird D, Fei Q, Scale-Up Considerations for Biofuels, *Biotechnology for Biofuel Production and Optimization*, pp. 513-537, 2016, DOI: https://doi.org/10.1016/B978-0-444-63475-7.00020-0

[17] Fernando J. R-Squared: Definition, Calculation Formula, Uses, and Limitations, https://www.investopedia.com/terms/r/r-squared.asp#:~:text=R%2Dsquared%20(R2),variable%20in%20a%20regression%20model (accessed on Feb. 12 2023)

[18] Jacob S, Nair A B, Shah J, Emerging role of nanosuspensions in drug delivery systems, *Biomaterials Research,* vol. 24, no. 3, 2020, DOI: https://doi.org/10.1186/s40824-020-0184-8

[19] Aslan N, Cebeci Y, Application of Box–Behnken design and response surface methodology for modeling of some Turkish coals, *Fuel*, vol. 86, no. 1-2, pp. 90-97, 2007, DOI: https://doi.org/10.1016/j.fuel.2006.06.010

[20] Costa P, Lobo JMS, Modeling and comparison of dissolution profiles, *European Journal of Pharmaceutical Sciences*, vol. 13, no. 2, pp. 123-133, 2001, DOI: https://doi.org/10.1016/S0928-0987(01)00095-1

[21] Rabindranath P, Chakraborty M, Rabindra D, Gupta BK, *In-vitro In-vivo correlation* (IVIVC) study of leflunomide loaded microspheres, *International Journal of Pharmacy and Pharmaceutical Sciences,* vol. 1, no. 1, pp. 165-170, 2009, URL: https://innovareacademics.in/journal/ijpps/Vol1Suppl1/266.pdf

[22] Herbert JM, Dol F, Bernat A, Falotico R, Lalé A, Savi P, The antiaggregating and antithrombotic activity of clopidogrel is potentiated by aspirin in several experimental models in the rabbit, *Thrombosis and Haemostasis,* vol. 80, no. 3, pp. 512-518, 1998, URL: https://pubmed.ncbi.nlm.nih.gov/9759636/

[23] Momi S, Pitchford SC, Alberti PF, Minuz P, Del Soldato P, Gresele P, Nitroaspirin plus clopidogrel versus aspirin plus clopidogrel against platelet thromboembolism and intimal thickening in mice, *Thrombosis and Haemostasis,* vol. 93, no. 3, pp. 535-543, 2005, DOI: https://doi.org/10.1160/TH04-07-0464

[24] Hornok V, Serum Albumin Nanoparticles: Problems and Prospects, *Polymers (Basel)*, vol. 13, no. 21, 2021, DOI: https://doi.org/10.3390/polym13213759

[25] Jenita JJL, Tibrewal R, Rathore SS, Manjula D, Barnabas W, Mahesh AR, Formulation and optimization of albumin nanoparticles loaded Ivabradine hydrochloride using response surface design, *Journal of Drug Delivery Science and Technology*, vol. 63, 2021, DOI: https://doi.org/10.1016/j.jddst.2021.102461

[26] The ANOVA table (SS, df, MS, F) in two-way ANOVA, KNOWLEDGEBASE - ARTICLE #1909, URL: https://www.graphpad.com/support/faq/the-anova-table-ss-and-df-in-two-way-anova/#:~:text=Mean%20squares,to%20compute%20the%20MS%20value (accessed on Mar. 11 2023)

[27] Jun J Y, Nguyen H H, Paik S, Chun H S, Kang B, Ko S, Preparation of size-controlled bovine serum albumin (BSA) nanoparticles by a modified desolvation method, *Food Chemistry*, vol.127, no. 4, pp. 1892-1898, 2011, DOI: https://doi.org/10.1016/j.foodchem.2011.02.040

[28] Shen S, Wu Y, Liu Y, Wu D, High drug-loading nanomedicines: progress, current status, and prospects, *International Journal of Nanomedicine*, vol. 12, pp. 4085-4109, 2017, DOI: https://doi.org/10.2147/IJN.S132780

[29] Zapadka KL, Becher FJ, Gomes dos Santos AL, Jackson SE, Factors affecting the physical stability (aggregation) of peptide therapeutics, *Interface Focus,* vol. 7, no. 6, pp. 1-18, 2017, DOI: https://doi.org/10.1098/rsfs.2017.0030

[30] Honary S, Zahir F, Effect of zeta potential on the properties of nano-drug delivery systems-a review (Part 1), *Tropical Journal of Pharmaceutical Research,* vol. 12, no. 2, pp. 255-264, 2013, DOI: https://doi.org/10.4314/tjpr.v12i2.19

[31] Clopidogrel, DrugFuture, Chemical Index Database, https://www.drugfuture.com/chemdata/clopidogrel.html (accessed on Jan. 2 2023)

[32] Mircioiu C, Voicu V, Anuta V, et al, Mathematical Modeling of Release Kinetics from Supramolecular Drug Delivery Systems, *Pharmaceutics*, vol. 11, no. 3, pp. 140, 2019, DOI: https://doi.org/10.3390/pharmaceutics11030140

[33] Dash S, Murthy PN, Nath L, Chowdhury P, Kinetic modeling on drug release from controlled drug delivery systems. *Acta Poloniae Pharmaceutica,* vol. 67, no. 3, pp. 217-223, 2010, URL: https://www.ptfarm.pl/pub/File/Acta_Poloniae/2010/3/217.pdf